2009

NOS-Based Biopolymers: Towards Novel Thromboresistant No-Release Materials

Charbel Abou diwan
Cleveland State University

NOS-BASED BIOPOLYMERS; TOWARDS NOVEL THROMBORESISTANT NO-RELEASE MATERIALS

CHARBEL ABOU DIWAN

Bachelor of Science in Medical Laboratory Technology

American University of Beirut

September, 2000

Masters of Science in Clinical Chemistry

University of Westminster

September, 2003

Submitted in partial fulfillment of the requirements for the degree of

DOCTOR OF PHILOSOPHY IN CLINICAL-BIOANALYTICAL CHEMISTRY

at the

CLEVELAND STATE UNIVERSITY

May, 2009

This dissertation has been approved for the Department of Chemistry and the College of Graduate Studies by:

_____

Dissertation Committee Chairperson, Dr. Mekki Bayachou

Department of Chemistry, Cleveland State University

_____

Dissertation Committee Member, Dr. David Anderson
Department of Chemistry, Cleveland State University

_____

Dissertation Committee Member, Dr. Xue-Long Sun
Department of Chemistry, Cleveland State University

_____

Dissertation Committee Member, Dr. Yan Xu
Department of Chemistry, Cleveland State University

_____

Dissertation Committee Member, Dr. Gary Wnek
Department of Macromolecular Science and Engineering, Case Western Reserve University

DEDICATION AND ACKNOWLEDGMENTS

I would like to acknowledge and extend my heartfelt gratitude to the people who made all of this possible: My mentor, Dr. Mekki Bayachou, for all the help, guidance, and motivation throughout those years. My committee members, Dr. Gary Wnek, Dr. David Anderson, Dr. Yan Xu, and Dr. Xue-long Sun for serving on my dissertation committee. The faculty of the Department of Chemistry at Cleveland State University for all their help. I would like to thank my fellow Bayachou lab members for their assistance through all the phases of my PhD. I would like to specifically thank Dr. Jean Boutros for his help and friendship throughout those years.

I dedicate this thesis to my family; my wife Marcelle for all her support, my parents Hikmat and Mountaha Abou Diwan for believing in me.

NOS-BASED BIOPOLYMERS; TOWARDS NOVEL THROMBORESISTANT NO-RELEASE MATERIALS

CHARBEL ABOU DIWAN

ABSTRACT

Nitric Oxide releasing biopolymers have the potential to prolong vascular graft and stent potency without adverse systemic vasodilation. It was reported in literature that eNOS-overexpressing endothelial cell seeding of synthetic small diameter vascular grafts decreased human platelet aggregation by 46% and bovine aortic smooth muscle cell proliferation by 67.2% *in vitro*. We hypothesized that incorporating the enzyme nitric oxide synthase (NOS) in biocompatible polymeric matrix will provide a source of NO that utilizes endogenous compounds to maintain an unlimited supply of NO. To test this hypothesis, we have incorporated the enzyme nitric oxide synthase into a polyethyleneimine film using a layer-by-layer electrostatic deposition. This approach will provide a source of NO that utilizes endogenous compounds available in the blood matrix to maintain a constant supply of NO at the blood/device interface. When coated onto the surface of various blood-contacting implantable medical devices, it will provide NO

fluxes at levels equal or greater than the normal endothelial cells, and for extended time periods. This configuration will help solve the issues of both thrombosis and stenosis that occur as side effects for several types of biomedical implants.

Our results indicate a proof of principle of a new approach for making antithrombotic coatings for medical devices and implants based on NO release. We have demonstrated that NOS-based polymetric films successfully generate NO under physiologic conditions at small levels equal to and higher than those observed for endothelial cells. The level of NO release can be fine-tuned through varying the number of NOS layers in the film buildup. We have shown that NO fluxes from our NOS-based PEI films are sustained for prolonged periods of time, which has the potential of producing efficient, short and long-term, antithrombotic coatings for medical devices and blood-contacting tools such as stents and catheters. We also show that NO release from these coatings successfully decrease platelet adhesion at the surface by 60%. This, and other properties are key for the desired thromboresistivity needed for blood-contacting medical devices.

TABLE OF CONTENTS

LIST OF TABLES

LIST OF FIGURES

CHAPTER I

INTRODUCTION

1.1 BIOCOMPATIBILITY ISSUES OF IMPLANTABLE MEDICAL DEVICES

The thrombogenic nature of various polymeric materials utilized to prepare various blood-contacting and implantable medical devices such as vascular grafts, intravascular catheters and sensors, coronary artery and vascular stents, even if labeled as *biocompatible*, can cause serious complications in patients [2]. Upon introduction of a foreign material into the blood stream, key proteins of the coagulation cascade (fibrinogen, and von Willebrand's factor) adsorb to the surface, followed by platelet adhesion and activation, leading to fibrin and thrombus formation at the surface (Figure 1.1) [3].

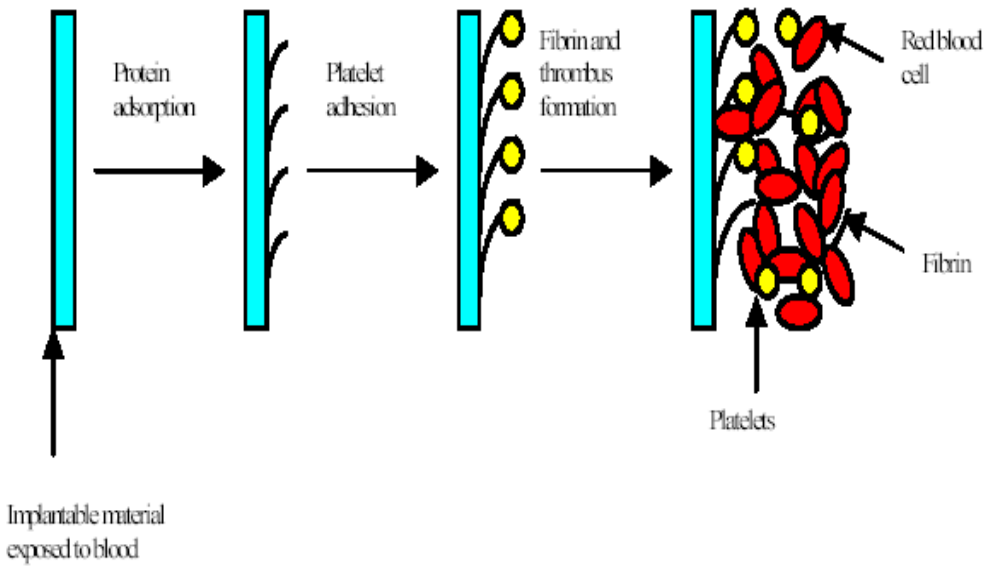

Figure 1.1: Illustration showing thrombus formation at the surface of implantable medical devices. Upon exposure to blood, protein adsorption occurs, followed by platelet adhesion at the surface. Platelet activation leads to thrombus formation at the surface.

An anti-coagulation regiment, with the adverse effects associated with long term use, is typically required to clinically reduce the risk of thrombus formation [4]. Thrombus formation and generation involves two synergistic events; a cGMP-dependant mechanism that involves platelet activation, adhesion and aggregation [5], and fibrin formation resulting from the binding of bivalent fibrinogen to glycoprotein IIb/IIIa [6].

In addition to thrombus formation, certain medical devices, during the implantation process can damage the endothelium lining of blood vessels, leading to smooth muscle cell proliferation, and ultimately cause vascular stenosis via neointimal hyperplasia [7,8]. Further more, bacterial adhesion at the material surface of medical devices leads to device-associated infections [9]. Early bacterial adhesion is mediated by reversible bacteria-substrate interactions, followed by irreversible molecular bridging at longer times [10]. Upon adhesion, certain bacteria are capable of secreting an exopolysaccharide matrix forming a protective biofilm that retains nutrients and protects the bacteria from the host immune response. Biofilms provides bacterial resistance to traditional antibiotic therapies [11].

Implantation into subcutaneous tissues subjects implants to an inflammatory response involving the release of fluid and plasma proteins followed by the recruitment of leukocytes at the implant site. Neutrophils and monocytes migration and adhesion to the implant surface initiates phagocytosis. After the initial inflammatory response, a more chronic response involves a sustained inflammation at the implant site involving the recruitment of macrophages, monocytes, and lymphocytes. Eventually, a fibrous capsule composed mainly of macrophages and collagen is formed around the implanted device.

1.2 THE PROTECTIVE ROLE OF ENDOGENOUS NITRIC OXIDE (NO)

Endogenous NO production at low concentrations (nanomolar) plays a critical role in the regulation of vascular hemostasis [12]. Endothelium derived NO production inhibits platelet adhesion [13], aggregation [14], and their further recruitment to the growing thrombus [15]. NOS inhibition is associated with the shortening of bleeding times in healthy volunteers [16], and platelet accumulation in the vasculature of animals [17]. *In vivo* studies involving production of high levels of NO

from iNOS showed the ability to prevent platelet adhesion [18]. NO, prostacyclin, and ecto-AD(T)Pase are potent inhibitors of platelet function that are produced by an intact endothelium [19]. Nitric oxide diffuses into platelets stimulating cGMP production by soluble guanylyl cyclase causing a decrease in cytosolic Ca^{2+} levels by directly inhibiting voltage-gated Ca^{2+} channels [20]. Calcium acts as an important second messenger with an intracellular concentration 50-100nM in resting platelets. Upon platelet activation, intracellular calcium concentrations can rise up to 1mM [21], triggering a cascade of events that leads to platelet aggregation.

The regulatory effect of NO on cGMP and cGMP-dependant protein kinases was reported by a significant increase in platelet aggregation in the presence of guanylyl cyclase inhibitors [22,23], and by the potentiation of anti-platelet effects in the presence of cGMP phosphodiesterase inhibitors [24]. Reduction in Ca^{2+} levels via a cGMP dependant mechanism inhibits thrombin mediated activation of phosphoinositide 3-kinase (PI-3 kinase) [25,26] leading to a suppression of the conformational change of glycoprotein IIb/IIIa required for fibrinogen binding [27], which decreases the number and affinity of fibrinogen binding sites on the platelet surface [28]. cGMP is also

involved in increasing intracellular cAMP indirectly by inhibiting the phosphodiesterase III (PDE III) dependant degradation of cAMP [29]. Increased levels of cAMP has been associated with decreased levels of intracellular Ca^{2+} flux [30,31]. In addition cGMP down-regulates protein kinase C leading to regulation of the surface expression of α granule protein P-selectin, a mediator of platelet adhesion [32].

There have been various reports indicating NO release from resting [33] and aggregating platelets [24,34]. NO levels from activated human platelets have been indirectly measured and is estimated at 11.2 $pmol.min^{-1}/10^{8}$ cells [33]. NO temporarily inactivates platelets in the close proximity of the endothelium [35-37]. This inhibition is short-lived and NO is rapidly scavenged by oxygen and hemoglobin in plasma [38,39].

NO is produced by macrophages as part of the natural immune response to bacterial infections [40,41]. NO is shown to mediate the inhibition of a wide variety of Gram-negative and Gram-positive bacterial species [42], as well as reducing bacterial adhesion [43].

1.3 THE ROLE OF NO-RELEASING MATERIALS AS COATINGS FOR IMPLANTABLE MEDICAL DEVICES

Considerable research is being focused on improving the surface chemistry of materials used as outer coatings of implantable medical devices [3]. NO releasing polymers have the potential to be effective in preventing platelet adhesion, activation, and aggregation onto the surfaces, therefore reducing the risk of thrombus formation at these surfaces. They have the potential to prolong vascular graft and stent potency without adverse systemic vasodilation [44]. NO exhibits a short half-life <1s in the presence of oxygen and hemoglobin, there is no systemic effects that can be caused by the NO-releasing coatings because any NO released will be rapidly consumed locally near the surface of the device [45]. Numerous approaches are currently being investigated in an attempt to develop polymeric materials that are more blood-compatible. In general, these approaches can be categorized into two main trends: first, methods that mimic endothelial cells anti-thrombogenic properties [46-50], and, second, methods that use modified chemical surfaces and added moieties that exhibit decreased protein and cell adhesion [1]. Prevention of protein adhesion *in vivo* is generally difficult to achieve, therefore the other approach, which aims at the development of NO-

releasing surfaces akin to native endothelial cells, appears more promising. Nitric oxide, thrombomodulin, prostacyclin, and heparans contribute to the non-thrombogenic properties of the endothelial cells [2,51]. Polymers that possess chemical platforms with the ability of releasing NO have been shown to be more thromboresistant. A potential solution can be found in polymeric materials that are capable of releasing low levels of nitric oxide at the blood/polymer interface.

1.4 CLASSES OF NO-RELEASING MATERIALS

Two classes of NO-releasing materials have been explored (Figure 1.2). N-diazeniumdiolate based NO-releasing polymers [52-56], and Nitrosothiol-based NO-releasing polymers [57-61] .

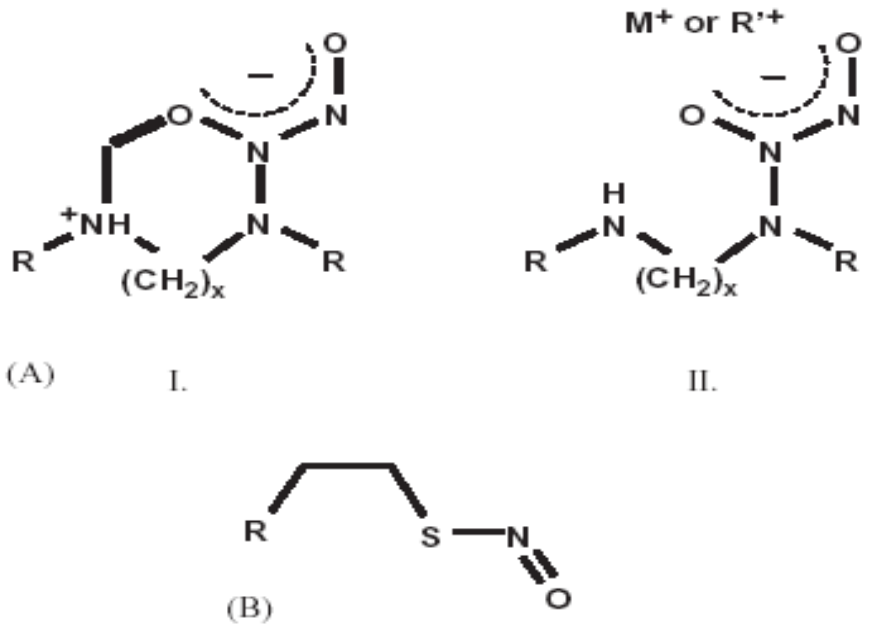

Figure 1.2: Generic structure of (A) Diazeniumdiolates (I) zwitterionic, (II) cation stabilized. (B) S-Nitrosothiol. Adapted from [1]

1.4.1 N-Diazeniumdiolates

N-diazeniumdiolates are inorganic NO donors formed by the reaction of a secondary amine structure with 2 moles of NO gas under high pressure, creating a relatively stable adduct structure [62-64]. A countercation is required to fulfill electroneutrality of the negatively charged diazeniumdiolate adduct, leading to zwitterionic molecules [1]. Three general structural types of diazeniumdiolates have been outlined for preparing diazeniumdiolates based NO-releasing polymers: Dispersed non-covalently bound small molecules where the diazeniumdiolate group is attached to amines in low molecular weight compounds; covalently bound diazeniumdiolates group to polymeric side chains or to the polymeric backbone [56].

Since this initial work, additional methods for preparing NO-releasing polymers utilizing diazeniumdiolates as NO donors were described by both Pulfer et al. [55] and Zhang et al. [54] Pulfer and co-workers developed NO releasing PEI microspheres that were entrapped into vascular grafts pores [55]. Zhang and co workers prepared diazeniumdiolate nanoparticles by reacting NO with alkylamines tethered onto the surface of fumed silica particles (7-10nm diameter) [54].

Diazeniumdiolated-dimethylhexyldiamine (DMHD/N_2O_2) were used to prepare NO-releasing polymers as coatings for oxygen sensors [65], and extracorporeal circuits [46]. In other studies, diethylenetriamine diazeniumdiolate (DETA/ N_2O_2) was embedded into ethylene-vinyl acetate [66,67]. In other work, diazeniumdiolate-spermine (SPER/N_2O_2) was incorporated into a biodegradable polymer used to construct jugular vascular grafts [68]. Although initial studies proved the worthiness of such materials, leaching of the water-soluble diazeniumdiolates was shown to form nirtosoamine, a well known class of carcinogens, due to the oxidation of local NO to an NO^+ intermediates that form RN-NO species upon reactions with amine compounds [69]. To counter this problem, more lipophilic discrete dialkyldiamine diazeniumdiolates such as dibutylhexyldiamine diazneniumdiolate (DHBD/N_2O_2) were prepared that have higher octanol/water partition coefficients and would be more likely to stay in polymer phase, even if nitrosoamine formation occurs [44]. The use of a diazeniumdiolate substrate that would be benign upon leaching was used as another method to avoid the buildup of carcinogenic species. The amino acid L-proline was used to prepare the anionic diazeniumdiolate of proline (PROLI/N_2O_2), and thus the nitrosamime form of proline is non- carcinogenic and would therefore be

harmless to the patient [70]. The covalent attachement of diazeniumdiolate moiety to the polymer backbone was used to prevent leaching of any potentially carcinogenic species. Diazeniumdiolated silicone rubbers were prepared by the use of diamino- and triamino-alkyltrimethoxysilanes cross-linkers with hydroxyl terminated polydimethylsiloxanes followed by reaction with NO [48]. Anionic diazeniumdiolated polymethacrylates were prepared by copolymerizing various secondary amine-containing monomers with methyl-methacrylate [71]. A protected diazeniumdiolated poly(vinyl chloride) was synthesized by using the O(2)-alkylated diazeniumdiolate of piperazine as a linker for incorporation of the diazeniumdiolate onto the polymeric backbone [72]. Alternative matrices for the incorporation and covalent attachement of diazeniumdiolates have been investigated and include sol-gels and hydrogel dressings. Discrete diazeniumdiolates (DETA/N_2O_2), dipropylenetriamine diazeniumdiolates (DPTA/N_2O_2), and DPTA/N_2O_2-g-dextran, were suspended in a hydrogel matrix [73]. The synthesis of sol gel materials by reaction of alkoxylsilanes with alkyltrimethoxysilanes followed by exposure to NO has been reported [74]. In addition, hydrogels as NO carriers were prepared by reacting polyethylene glycol N-hydroxysucinimide monoacrylate with poly L-lysine and then

dissolving the product in water followed by the exposure to NO [57], and by the reaction of NO with cross-linked poly(vinyl-acetate) modified with amine groups [75].

1.4.2 S-Nitrosothiols

The second class of NO donors are S-nitrosothiols; they are thought to serve as NO reservoirs and transporters within biological systems [76]. S-Nitroso-albumin and S-nitrosoglutathione are the most abundant naturally occurring S-nitrosothiols circulating in blood [77]. The cleavage of the S-NO bond releases NO by three known mechanisms [78]: copper mediated decomposition[79], the direct reaction of ascorbate [80], and photolytic decomposition [81]. S-nitrosothiols have been covalently linked to the polymer to prevent leaching of the donor or reaction byproducts. NO releasing hydrogels were prepared by linking cysteine to Polyethylene glycol (PEG) and reacting the resultant copolymers with sodium nitrite to form S-nitrosocysteine groups [57]. The S-nitrosothiol (GSNO) and S-nitroso-N-acetylcysteine (SNAC) were blended into poly(ethylene oxide) and poly(propylene oxide) copolymers or PEG for targeted deliver of NO in biomedical applications [58,59]. In

addition, S-nitrosothiols can be tethered to the surface of polymer fillers. S-nitroso-N-acetylpenicillamine (SNAP) was tethered to the surface of 7-10nm diameter fumed silica particles [82].

The greatest limitation of these approaches is that they are a finite reservoir of NO, which will limit their potential use in more permanent types of implants, and the NO fluxes achieved so far are lower than NO released from endothelial cells [1]. Studies have shown that stimulated human endothelial cells continuously generate NO at a level of ca. $4x10^{-10}$ $mol.cm^{-2}.min^{-1}$ [83].

1.5 NOS BASED NO-RELEASING MATERIALS

The logical alternative is then to explore approaches that would lead to materials with the ability to sustain NO generation for longer durations. Some current developments include materials that utilize endogenous NO donors such as S-nitrosothiols and nitrite to generate NO [84-86]. Though these approaches display potential, with their current limitations, it is not likely to overcome the complexity of the biocompatibility issues of medical devices.

Developing a NO-releasing surface that closely resembles the endothelium is the key to achieving better thromboresistivity. The endothelial isoform of the enzyme Nitric Oxide Synthase, eNOS, is a key component of the endothelial cell lining. It was reported that eNOS-overexpressing endothelial cells seeding of synthetic small diameter vascular grafts decreases human platelet aggregation by 46% and bovine aortic smooth muscle cell proliferation by 67.2% *in vitro* [87]. NO releasing materials using Polyethyleneimine (PEI), a biocompatible polymer [88], has been reported in literature [55,89,90]. In our lab, NO was successfully generated from the enzyme Nitric Oxide Synthase embedded in bilayered cast film of didodecyldimethylammonium bromide surfactant [91]. We have incorporated the oxygenase domain of the enzyme Nitric Oxide Synthase (NOSoxy) in a Polyethyleneimine polymeric matrix by means of layer-by-layer electrostatic adsorption [92,93] to construct a multi-component protein film that mimics the NO-generating behavior of the endothelial cell lining. We have demonstrated that our films provide a source of NO that utilizes endogenous compounds to maintain a continuous supply of NO at levels that are in the same range as that of endothelial cells [94].

1.6 REFERENCES

1. Frost MC, Reynolds MM, Meyerhoff ME. Polymers incorporating nitric oxide releasing/generating substances for improved biocompatibility of blood-contacting medical devices. Biomaterials 2005;26:1685-1693.
2. Coleman RW. Mechanism of thrombus formation and dissolution. Cardiovascular Pathology 1993;2:23S-31S.
3. Frost M, Meyerhoff ME. In vivo chemical sensors: tackling biocompatibility. Anal Chem 2006;78(21):7370-7.
4. Majerus PWB, G.J. Miletich, J.P.Tollefsen, D.M. Anticoagulant, thrombolytic and anitplatelet drugs. New York: Pergamon Press; 1991.
5. Cheung PY, Salas E, Schulz R, Radomski MW. Nitric oxide and platelet function: implications for neonatology. Semin Perinatol 1997;21(5):409-17.
6. Freedman JE, Loscalzo J, Barnard MR, Alpert C, Keaney JF, Michelson AD. Nitric oxide released from activated platelets inhibits platelet recruitment. J Clin Invest 1997;100(2):350-6.

7. Hoffmann R, Mintz GS. Coronary in-stent restenosis - predictors, treatment and prevention. Eur Heart J 2000;21(21):1739-49.
8. Roy-Chaudhury P, Kelly BS, Miller MA, Reaves A, Armstrong J, Nanayakkara N, et al. Venous neointimal hyperplasia in polytetrafluoroethylene dialysis grafts. Kidney Int 2001;59(6):2325-34.
9. Vacheethansanee KM, RE. Nonspecific Staphylococcus epidermidis adhesion: contributions of biomaterial hydrophobicity and charge. In: An YH, Friedman RJ, editors. Handbook of bacterial adhesion: principles, methods, and applications. Totowa, NJ: Humana Press; 2000. p. 74.
10. An YH, Friedman RJ. Concise review of mechanisms of bacterial adhesion to biomaterial surfaces. J Biomed Mater Res 1998;43(3):338-48.
11. Smith AW. Biofilms and antibiotic therapy: is there a role for combating bacterial resistance by the use of novel drug delivery systems? Adv Drug Deliv Rev 2005;57(10):1539-50.
12. Walford G, Loscalzo J. Nitric oxide in vascular biology. J Thromb Haemost 2003;1(10):2112-8.

13. Ignarro L. Biological actions and properties of endothelium-derived nitric oxide formed and released from artery and vein. Circ Res 1989;65:1-21.
14. Azuma HI, M. Sekizaki, S. Endothelium-dependant inhibition of platelet aggregation. Br J Pharmacol 1986;88:411-5.
15. Freedman JE, Sauter R, Battinelli EM, Ault K, Knowles C, Huang PL, et al. Deficient platelet-derived nitric oxide and enhanced hemostasis in mice lacking the NOSIII gene. Circ Res 1999;84(12):1416-21.
16. Simon DI, Stamler JS, Loh E, Loscalzo J, Francis SA, Creager MA. Effect of nitric oxide synthase inhibition on bleeding time in humans. J Cardiovasc Pharmacol 1995;26(2):339-42.
17. Stagliano NE, Zhao W, Prado R, Dewanjee MK, Ginsberg MD, Dietrich WD. The effect of nitric oxide synthase inhibition on acute platelet accumulation and hemodynamic depression in a rat model of thromboembolic stroke. J Cereb Blood Flow Metab 1997;17(11):1182-90.
18. Yan ZQ, Yokota T, Zhang W, Hansson GK. Expression of inducible nitric oxide synthase inhibits platelet adhesion and restores blood flow in the injured artery. Circ Res 1996;79(1):38-44.

19. Battinelli EM, Loscalzo J. Nitric Oxide and platelet-mediated hemostasis. In: Loscalzo J, Vita JA, editors. Nitric oxide and the cardiovascular system. HUmana, Totowa, NJ; 2000. p. 123-138.
20. Trepakova ES, Cohen RA, Bolotina VM. Nitric oxide inhibits capacitative cation influx in human platelets by promoting sarcoplasmic/endoplasmic reticulum Ca2+-ATPase-dependent refilling of Ca2+ stores. Circ Res 1999;84(2):201-9.
21. Kroll MH, Schafer AI. Biochemical mechanisms of platelet activation. Blood 1989;74(4):1181-95.
22. Moro MA, Russel RJ, Cellek S, Lizasoain I, Su Y, Darley-Usmar VM, et al. cGMP mediates the vascular and platelet actions of nitric oxide: confirmation using an inhibitor of the soluble guanylyl cyclase. Proc Natl Acad Sci USA 1996;93:1480-1485.
23. Rao GH, Krishnamurthi S, Raij L, White JG. Influence of nitric oxide on agonist-mediated calcium mobilization in platelets. Biochem Med Metab Biol 1990;43(3):271-5.
24. Radomski MW, Palmer RM, Moncada S. An L-arginine/nitric oxide pathway present in human platelets regulates aggregation. Proc Natl Acad Sci U S A 1990;87(13):5193-7.

25. Pigazzi A, Heydrick S, Folli F, Benoit S, Michelson A, Loscalzo J. Nitric oxide inhibits thrombin receptor-activating peptide-induced phosphoinositide 3-kinase activity in human platelets. J Biol Chem 1999;274(20):14368-75.

26. Zhang J, Shattil SJ, Cunningham MC, Rittenhouse SE. Phosphoinositide 3-kinase gamma and p85/phosphoinositide 3-kinase in platelets. Relative activation by thrombin receptor or beta-phorbol myristate acetate and roles in promoting the ligand-binding function of alphaIIbbeta3 integrin. J Biol Chem 1996;271(11):6265-72.

27. Michelson AD, Benoit SE, Furman MI, Breckwoldt WL, Rohrer MJ, Barnard MR, et al. Effects of nitric oxide/EDRF on platelet surface glycoproteins. Am J Physiol 1996;270(5 Pt 2):H1640-8.

28. Mendelsohn ME, O'Neill S, George D, Loscalzo J. Inhibition of fibrinogen binding to human platelets by S-nitroso-N-acetylcysteine. J Biol Chem 1990;265(31):19028-34.

29. Bowen R, Haslam RJ. Effects of nitrovasodilators on platelet cyclic nucleotide levels in rabbit blood; role for cyclic AMP in synergistic inhibition of platelet function by SIN-1 and prostaglandin E1. J Cardiovasc Pharmacol 1991;17(3):424-33.

30. Fischer TH, White GC, 2nd. Partial purification and characterization of thrombolamban, a 22,000 dalton cAMP-dependent protein kinase substrate in platelets. Biochem Biophys Res Commun 1987;149(2):700-6.

31. Geiger J, Nolte C, Walter U. Regulation of calcium mobilization and entry in human platelets by endothelium-derived factors. Am J Physiol 1994;267(1 Pt 1):C236-44.

32. Murohara T, Parkinson SJ, Waldman SA, Lefer AM. Inhibition of nitric oxide biosynthesis promotes P-selectin expression in platelets. Role of protein kinase C. Arterioscler Thromb Vasc Biol 1995;15(11):2068-75.

33. Zhou Q, Hellermann GR, Solomonson LP. Nitric oxide release from resting human platelets. Thromb Res 1995;77(1):87-96.

34. Malinski T, Radomski MW, Taha Z, Moncada S. Direct electrochemical measurement of nitric oxide released from human platelets. Biochem Biophys Res Commun 1993;194(2):960-5.

35. West JB. Hemostasis. twelfth ed. Baltimore: Williams & WilkinsI; 1989.

36. de Graaf JC, Banga JD, Moncada S, Palmer RM, de Groot PG, Sixma JJ. Nitric oxide functions as an inhibitor of platelet adhesion under flow conditions. Circulation 1992;85(6):2284-90.
37. MacAllister RJ, Vallance P. The L-arginine nitric oxide pathway in the human cardiovascular system. J Int Fed Clin Chem 1996;8:152-158.
38. Moncada SP, R.M.J. Biosynthesis and actions of nitric oxide. Semin Perinatol 1991;15:16-19.
39. Radomski MWM, S. The biological and pharmacological role of nitric oxide in platelet function. Adv Exp Med Biol 1993;344:255-261.
40. Fang FC. Perspectives series: host/pathogen interactions. Mechanisms of nitric oxide-related antimicrobial activity. J Clin Invest 1997;99(12):2818-25.
41. MacMicking J, Xie QW, Nathan C. Nitric oxide and macrophage function. Annu Rev Immunol 1997;15:323-50.
42. Raulli R, McElhaney-Feser G, Hrabie JA, Cihlar RL. Antimicrobial properties of nitric oxide using diazeniumdiolates as the nitric oxide donor. Recent Res Devel Microbiol 2002;6:177-83.

43. Nablo BJ, Chen TY, Schoenfisch MH. Sol-gel derived nitric-oxide releasing materials that reduce bacterial adhesion. J Am Chem Soc 2001;123(39):9712-3.

44. Batchelor MMR, S.L. Fleser, P.S. Nuthaki, V.K. Callahan, R.E. Shanley, C.J. Politis, J.K.Elmore, J. Merz, S.I. Meyerhoff, M.E. More lipophilic dialkyldiamine-based diazeniumdiolates: synthesis, characterization, and application in preparing thromboresistant nitric oxide release polymeric coatings. J Med Chem 2003;46:5153-5161.

45. Kelm M, Yoshida K. In: Feelisch M, Stamler JS, editors. Methods in Nitric Oxide Research. New York: John Wiley; 1996. p. 47-58.

46. Annich GM, Meinhardt JP, Mowery KA, Ashton BA, Merz SI, Hirschl RB, et al. Reduced platelet activation and thrombosis in extracorporeal circuits coated with nitric oxide release polymers. Crit Care Med 2000;28(4):915-20.

47. Schoenfisch MHM, K.A. Rader, M.V. Baliga, N. Wahr, J.A. Meyerhoff, M.E. Improving the thromboresistivity of chemical sensors via nitric oxide release: fabrication and in vivo evaluation of NO-releasing oxygen-sensing catheters. Anal Chem 2000;72:1119-1126.

48. Zhang H, Annich GM, Miskulin J, Osterholzer K, Merz SI, Bartlett RH, et al. Nitric oxide releasing silicone rubbers with improved blood compatibility: preparation, characterization, and in vivo evaluation. Biomaterials 2002;23(6):1485-94.
49. Feng J, Chaikof EL. Reconstitution of thrombomodulin into polymerizable phospholipid vesicles. Polym Prepr 2000;41:1-7.
50. Bramford CHM, I.P. Al-Lamee, K.G. Paprotny, J.J. Modification of biomaterials to improve blood compatibility. Int J ArtifOrgans 1992;15:71-78.
51. Matkrides SCR, U.S. Overview of the endothelium. In: Loscalzo JS, A.I., editor. Thrombosis and hemorrhage. Baltimore: Williams & Wilkins; 1998. p. 295-306.
52. Polizzi MA, Stasko NA, Schoenfisch MH. Water-Soluble Nitric Oxide-Releasing Gold Nanoparticles. Langmuir 2007;23(9):4938-4943.
53. Shin JH, Metzger SK, Schoenfisch MH. Synthesis of Nitric Oxide-Releasing Silica Nanoparticles. J. Am. Chem. Soc. 2007;129(15):4612-4619.
54. Zhang H, Annich GM, Miskulin J, Stankiewicz K, Osterholzer K, Merz SI, et al. Nitric oxide-releasing fumed silica particles: synthesis,

characterization, and biomedical application. J Am Chem Soc 2003;125(17):5015-24.

55. Pulfer SKO, D. Smith, D.J. Incorporation of Nitric oxde-releasing crosslinked polyethyleneimine microspheres into vascular grafts. J Biomed Res 1997;37:182-189.

56. Smith DJ, Chakravarthy D, Pulfer S, Simmons ML, Hrabie JA, Citro ML, et al. Nitric oxide-releasing polymers containing the [N(O)NO]-group. J Med Chem 1996;39(5):1148-56.

57. Bohl KSW, J.L. Nitric oxide-generating polymers reduce platelet adhesion and smooth muscle proliferation. Biomaterials 2000;21:2273-2278.

58. Shishido SM, Seabra AB, Loh W, de Oliveira MG. Thermal and photochemical nitric oxide release from S-nitrosothiols incorporated into Pluronic F127 gel: potential uses for local and controlled nitric oxide release. Biomaterials 2003;24:3543-3553.

59. Shishido SM, de Oliveira MG. Polyethylene glycol matrix reduces the rates of photochemical and thermal release of nitric oxide from S-nitroso-N-acetylcysteine. Photochem Photobiol 2000;71:273-280.

60. Etchenique RF, M. Olabe, J.A. Photodelivery of nitric oxide from a nitrosothiol-derivatized surface. J Am Chem Soc 2000;122:3967-3968.

61. Wu Y, Rojas AP, Griffith GW, Skrzypchak AM, Lafayette N, Bartlett RH, et al. Improving blood compatibility of intravascular oxygen sensors via catalytic decomposition of S-nitrosothiols to generate nitric oxide in situ. Sensors and Actuators B: Chemical

Special Issue: 25th Anniversary of Sensors and Actuators B: Chemical 2007;121(1):36-46.

62. Drago R, Paulik F. The reaction of nitrogen(II) oxide with diethylamine. J Am Chem Soc 1960;82:96-8.

63. Drago R, Karstetter B. The reaction of nitrogen(ii) oxide with various primary and secondary amines. J Am Chem Soc 1961;83:1819-22.

64. Hrabie JA, Keefer LK. New nitric oxide-releasing zwitterions derived from polyamines. J Org Chem 1993;58:1472-6.

65. Schoenfisch MH, Mowery KA, Rader MV, Baliga N, Wahr JA, Meyerhoff ME. Improving the Thromboresistivity of Chemical Sensors via Nitric Oxide Release: Fabrication and in Vivo Evaluation of NO-Releasing Oxygen-Sensing Catheters. Anal. Chem. 2000;72(6):1119-1126.

66. Gabikian P, Clatterbuck RE, Eberhart CG, Tyler BM, Tierney TS, Tamargo RJ. Prevention of experimental cerebral vasospasm by intracranial delivery of a nitric oxide donor from a controlled-release polymer: toxicity and efficacy studies in rabbits and rats. Stroke 2002;33(11):2681-6.

67. Tierney TS, Clatterbuck RE, Lawson C, Thai QA, Rhines LD, Tamargo RJ. Prevention and reversal of experimental posthemorrhagic vasospasm by the periadventitial administration of nitric oxide from a controlled-release polymer. Neurosurgery 2001;49(4):945-51; discussion 951-3.

68. Chaux A, Ruan XM, Fishbein MC, Ouyang Y, Kaul S, Pass JA, et al. Perivascular delivery of a nitric oxide donor inhibits neointimal hyperplasia in vein grafts implanted in the arterial circulation. J Thorac Cardiovasc Surg 1998;115(3):604-12; discussion 612-4.

69. Mowery KA, Schoenfisch MH, Saavedra JE, Keefer LK, Meyerhoff ME. Preparation and characterization of hydrophobic polymeric films that are thromboresistant via nitric oxide release. Biomaterials 2000;21(1):9-21.

70. Saavedra JE, Southan GJ, Davies KM, Lundell A, Markou C, Hanson SR, et al. Localizing antithrombotic and vasodilatory activity with a novel, ultrafast nitric oxide donor. J Med Chem 1996;39(22):4361-5.
71. Parzuchowski PG, Frost MC, Meyerhoff ME. Synthesis and characterization of polymethacrylate-based nitric oxide donors. J Am Chem Soc 2002;124(41):12182-91.
72. Saavedra JE, Booth MN, Hrabie JA, Davies KM, Keefer LK. Piperazine as a Linker for Incorporating the Nitric Oxide-Releasing Diazeniumdiolate Group into Other Biomedically Relevant Functional Molecules. Journal of Organic Chemistry 1999;64(14):5124-5131.
73. Smith DJ, Simmons ML. Transdermal delivery of nitric oxide from diazeniumdiolates. J Control Release 1998;51(2-3):153-9.
74. Marxer SM, Rothrock AR, Nablo BJ, Robbins ME, Schoenfisch MH. Preparation of Nitric Oxide (NO)-Releasing Sol−Gels for Biomaterial Applications. Chemistry of Materials 2003;15(22):4193-4199.
75. Masters KS, Leibovich SJ, Belem P, West JL, Poole-Warren LA. Effects of nitric oxide releasing poly(vinyl alcohol) hydrogel dressings on dermal wound healing in diabetic mice. Wound Repair Regen 2002;10(5):286-94.

76. Jourd'heuil D, Hallen K, Feelisch M, Grisham MB. Dynamic state of S-nitrosothiols in human plasma and whole blood. Free Radic Biol Med 2000;28(3):409-17.

77. Tyurin VA, Tyurina YY, Liu SX, Bayir H, Hubel CA, Kagan VE. Quantitation of S-nitrosothiols in cells and biological fluids. Methods Enzymol 2002;352:347-60.

78. Williams DLH. The chemistry of S-nitrosothiols. Acc Chem Res 1999;32:689-76.

79. Dicks AP, Williams DL. Generation of nitric oxide from S-nitrosothiols using protein-bound Cu2+ sources. Chem Biol 1996;3(8):655-9.

80. Holmes AJ, Williams DL. Reaction of ascorbic acid with S-nitrosothiols: clear evidence for two distinct reaction pathways. Chem Soc Perkin Trans-2 2000;8:1639-44.

81. Singh RJ, Hogg N, Joseph J, Kalyanaraman B. Mechanism of nitric oxide release from S-nitrosothiols. J Biol Chem 1996;271(31):18596-603.

82. Frost MC, Meyerhoff ME. Controlled photoinitiated release of nitric oxide from polymer films containing S-nitroso-N-acetyl-DL-

penicillamine derivatized fumed silica filler. J Am Chem Soc 2004;126(5):1348-9.

83. Vaughn MW, Kuo L, Liao JC. Estimation of nitric oxide production and reaction rates in tissue by use of a mathematical model. Am J Physiol 1998;274(6 Pt 2):H2163-76.

84. Duan XL, R.S. Improved haemocompatibility of cysteine modified polymers via endogenous nitric oxide. Biomaterials 2002;23:1197-1203.

85. Oh BK, Meyerhoff ME. Spontaneous catalytic generation of nitric oxide from S-nitrosothiols at the surface of polymer films doped with lipophilic copper(II) complex. J Am Chem Soc 2003;125:9552-9553.

86. Oh BKM, M.E. Catalytic generation of nitric oxide from nitrite at the interface of polymeric films doped with lyophilic Cu(II)-complex: a potential route to the preparation of thromboresistant coatings. Biomaterials 2004;23:283-293.

87. Kader KN, Akella R, Ziats NP, Lakey LA, Harasaki H, Ranieri JP, et al. eNOS-overexpressing endothelial cells inhibit platelet aggregation and smooth muscle cell proliferation in vitro. Tissue Eng 2000;6(3):241-51.

88. Dong CH, Yuan XY, He MY, Yao KD. Preparation of PVA/PEI ultra-fine fibers and their composite membrane with PLA by electrospinning. Journal of Biomaterials Science-Polymer Edition 2006;17(6):631-643.
89. Zhou Z, Annich GM, Wu Y, Meyerhoff ME. Water-soluble poly(ethylenimine)-based nitric oxide donors: preparation, characterization, and potential application in hemodialysis. Biomacromolecules 2006;7(9):2565-74.
90. Bauer JA, Rao W, Smith DJ. Evaluation of linear polyethyleneimine/nitric oxide adduct on wound repair: therapy versus toxicity. Wound Repair Regen 1998;6(6):569-77.
91. Bayachou M, Boutros J. Manuscript in preparation.
92. Decher GH, J.D. Buildup of ultrathin multilayer films by a self-assembly process: II. Consecutive adsorption of anionic and cationic bipolar amphiphiles and polyelectrolytes on charged surfaces. Berichte der Bunsen-Gesellschaft 1991;95(11):1430-1434.
93. Lvov YA, K. Ichinose, I. Kunitake, T. Assembly of Multicomponent Protein Films by Means of Electrostatic Layer-by-Layer Adsorption. Journal of the American Chemical Society 1995;117(22):6117-23.
94. Abou Diwan C, Bayachou M. Manuscript in preparation.

CHAPTER II

LAYER-BY-LAYER ASSEMBLY OF PROTEIN FILMS

2.1 INTRODUCTION

The technique of ultrathin film assembly via alternate adsorption of oppositely charged polyions was developed a couple of decades ago. In 1991, the alternate adsorption of linear polycations and polyanions as a method for film assembly was first introduced by Decher and co-workers [1-9]. The basis of this method is the excessive adsorption at every stage of the polycation/polyanion assembly that leads to recharging of the outermost surface at during the film formation.

This methodology relies on the following principle: a negatively charged substrate surface is immersed in a cationic polyelectrolyte solution allowing the electrostatic adsorption of the polycationic layer. Since high

concentrations of polyelectrolytes are utilized, a number of cationic groups remain exposed and thus the surface charge is effectively reversed. After rinsing with water, the substrate is immersed in an anionic polyelectrolyte solution restoring the original surface charge. By repeating both steps, alternating multilayer assemblies are obtained with repeatable layer thickness (scheme 2.1) [10].

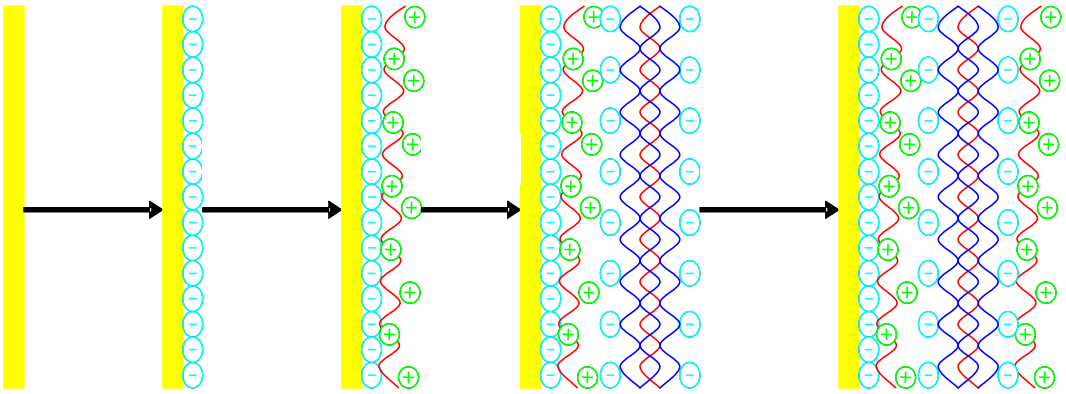

Figure 2.1: Scheme of layer-by-layer film assembly on a solid substrate by alternate adsorption of linear polycations and polyanions/negatively charged proteins.

Electrostatic layer-by-layer self-assembly has been applied to thin film coatings [6,11-13]. It allows the assembly of multilayers of materials on two-dimensional (2D) supports and on three-dimensional (3D) nanotemplates [14]. A variety of charged materials have been used in these 2D and 3D nanoassembly processes; they include linear polyectrolytes (synthetic and natural), enzymes, antibodies, viruses, and inorganic nanoparticles [14]. The resulting film architecture can be designed to meet different requirements such as biocompatibility, stability, and thickness, typically on the order of tens to hundreds of nanometers [14,15]. Layer-by-layer organized film assembly based on the alternate adsorption of oppositely charged macromolecules paves the way for a molecular architecture in the direction perpendicular to the solid support allowing for the design of films with nanometer resolution. Ultrathin films can be designed with definite molecular composition and ordered architecture in the range of 5-1000 nm with a precision better than 1nm [16]. Layer-by-layer assembly allows the control of the chemical composition of the films, which translates into control of the biological activity in biomedical applications. Ultrathin film coatings of a surface can maintain its original mechanical properties and structure [17].

For enzyme-based thin films, electrostatic adsorption seems to be one of the simplest ways for enzyme immobilization [15]. Other available methods of enzyme immobilization include physical adsorption [18], encapsulation [19], or covalent attachment [20,21]. However, these methods have disadvantages in terms of stability and low active site accessibility/activity. Site-targeted immobilization is complex but can provide enhanced activity if the immobilization does not interfere with enzyme function [22-24].

2.2 GENERALITY OF THE ASSEMBLY PROCEDURE

Layer-by-layer assembly of multilayered protein films has been performed by means of alternate electrostatic adsorption of either positively charged polyethyleneimine (PEI), poly(allylamine) (PAA), poly(dimethyldiallylammonium) (PDDA), or negatively charged poly(styrenesulfonate) (PSS), DNA, and heparin [8,10,25-38]. The pH of the protein component was set far from the isoelectric point in order to ensure sufficient charge under experimental conditions. The concentration range of aqueous proteins was 0.1 – 2 mg/ml or ~ 10^{-5}M. Examples of aqueous proteins used (table 2.1) were cytochrome c,

lysozyme, histone type YIII-S, myoglobin (Mb), pepsin, horseradish peroxidase (POD), hemoglobin, glycoamylase (GAM), concanavalin A (Con A), albumin [31], Glucose Oxidase [21,10,32], catalase, invertase, diaphorase [8,10], bacteriorhodopsin [37], and immunoglobulin (IgG) [33,39]. Protein stability can be affected by the surface structure of the solid support; therefore precursor films of alternate PEI/PSS were used as standard surfaces [8,10,29,40]. Solid surfaces are typically immersed in aqueous protein solutions or polyions for 20 minutes. Surfaces were then rinsed with water, and dried. To reach saturation of the adsorption process, the assembly process was carried out uninterrupted. A summary of the alternate adsorption of 18 water-soluble proteins in combination with oppositely charged polyions is listed in Table 2.1.

Protein	Molecular Weight	Isoelectric point	pH	Charge	Alternate with	Saturation time (min)	Protein monolayer mass coverage (mg/m^2)	Thickness of protein polyion bilayer [28]	Protein globule dimensions[28]
Cytochrome c	12400	10.1	4.5	+	PSS-	12	3.6	2.4 + 1.6	2.5 x 2.5 x 3.7
Lyzozyme	14000	11	4	+	PSS-	16	3.5	2.3 + 1.9	3.0 x 3.0 x 4.5
Histone f3	15300	11	7	+	PSS-	15	3.3	2.2 + 2.0	diameter 3.4
Myoglobin	17800	7.0	4.5	+	DNA, PSS-	12	6	4.0 + 2.0	2.5 x 3.5 x 4.5
Bacteriorhodopsin[36]	26000	6	9.4	-	PDDA+	5	7.5	5.0 + 1.0	ca 5.0
Pepsin	35000	1	6	-	PDDA+	20	4.5	3.0 + 0.6	diameter 3.0
Peroxidase	42000	8.0	4.2	+	PSS-	15	5.3	bilayer 3.5	diameter 3.5
Hemoglobin	64000	6.8	4.5 9.2	+ -	PSS- PEI+	16	26 27	17.5 + 3.0 bilayer 18.2	5.0 x 5.5 x 6.5
Albumin[31]	68000	4.9	8 3.9	- +	PDDA+ Heparin-	10 20	23 30	16.0 + 1.0 20.0 + 1.0	11.6 x 2.7 x 2.7
Glycoamylase	95000	4.2	6.8	-	PDDA, PEI+	15	4	2.6 + 0.5	diameter 6.3
Photosynt. RC	100000	5.5	8	-	PDDA+	15	13	9.0 + 1.0	13 x 7.0 x 4.0
Concanavalin	104000	5	7	-	PEI+	20	8.6	5.7 + 0.8	3.9 x 4.0 x 4.2
Alcohol dehydrogenase	141000	5.4	8.5	-	PDDA+	20	12.2	8.5 + 1.0	9.0 x 4.0 x 4.0
IgG[33]	150000	6.8	7.5	-	PSS-	60	15	10.0	14 x 10 x 5
Glucose Oxidase[32]	186000	4.1	6.8 9.2 6.5 6.5	- - - -	PDDA+ PEI+ PEI+ PAH+	15 15 15 15	12 16.6 51 12.6	bilayer 8.0 11.7 + 0.8 34.4 + 0.8 bilayer 8.4	diameter 8
Catalase	240000	5.5	9.2	-	PEI+	20	9.6	6.4 + 0.8	diameter 9.0
Invertase	270000	3.8	7.0	-	PDDA+	20	10.8	monolayer 7.3	diameter 8.6
Diaphorase	600000	5	8	-	PEI+	20	31	bilayer 21.0	diameter 11.5

Table 2.1: Protein-Polyion Alternate Multilayer Assembly

Unlimited cycling of proteins with oppositely charged polyions is reported. The mass changes were determined as a function of frequency shifts with Quartz Crystal Microbalance (QCM) measurments and was quite reproducible. An alternation with a polyion is required due to the unsuccessful attempts to grow protein films by the cyclic immersion of a substrate into a protein solution.

QCM, x-ray reflectivity, scanning electron microscopy, and surface plasmon resonance were the tools used to estimate protein layer thicknesses. These estimates correspond to known molecular dimensions of proteins obtained from crystallographic data and suggest the formation of relatively uniform monolayers. Parameters such as orientation, packing density, and hydration of proteins within the layer, might have significant influence on the thickness of the protein monolayer.

The multilayer formation as indicated in Figure 2.1 is quite general. The physical separation of the individual layers in the films is assumed on the basis of the regular, stepwise mass increase during the assembly. However, the layer separation between the proteins and the oppositely charged polyions may not be as definite, and the linear polyions would cover the protein surface and act as bridging molecules, to enhance protein stability.

Altering the pH around the isoelectric point allows the protein to be assembled with polyanions and polycations. The protein can be used at a pH above the isoelectric point (i.e. negatively charged) to assemble with polycations and at a pH below the isoelectric point (i.e. positively charged). Examples of both cases are hemoglogbin/PEI^{+}, hemoglobin/PSS^{-}, and albumin/PDDA, or $heparin^{-}$ multilayers (table 2.1). The layer-by-layer immobilization of proteins onto solid substrates with strong polyions (such as PSS, PEI, PDDA) renders it insoluble in a buffer for a pH range between 3 and 10. Immobilization of proteins with weak polyions renders it partially soluble in buffers with pH close to the isoelectric point of one of the components.

Lvov and co-workers demonstrate the dependence of QCM frequency shift on cycles of alternate Myoglobin (Mb) /Polystyrenesulfonate (PSS) adsorption. QCM shifts were proportional to the adsorbed mass at the surface of quartz crystals, and correspond to protein monolayer formation at every step of the film formation process [8,10]. Figure 2.2 represent the typical UV/vis spectra for a Mb/PSS film at consecutive steps of the assembly, with a linear increase in the Soret band absorbance (407nm) with the number of myoglobin layers in the film.

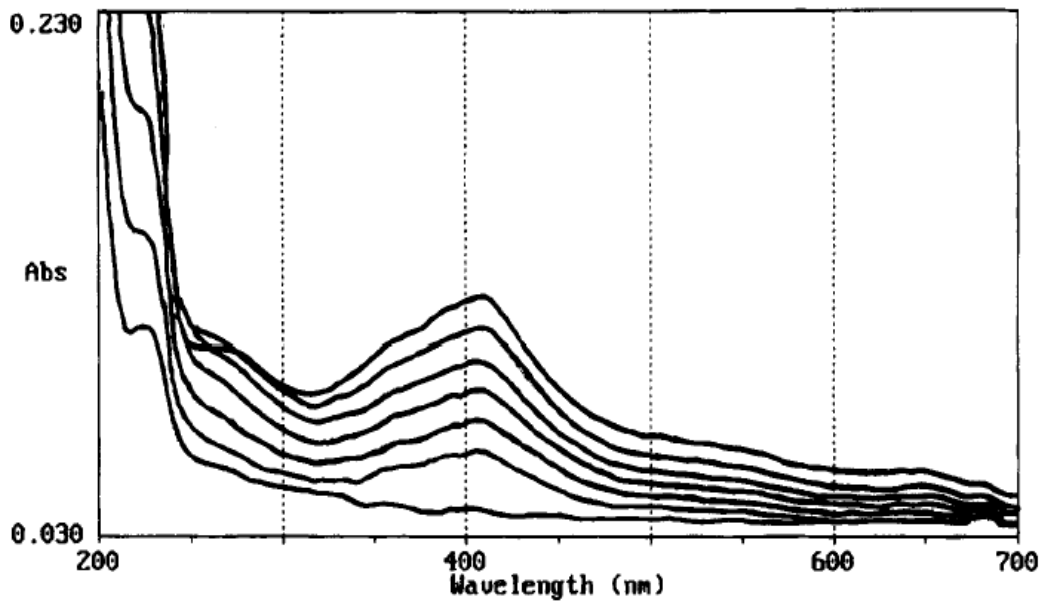

Figure 2.2: UV/vis spectra of Mb/PSS assembly. The lowest spectrum corresponds to a precursor film. The following spectra correspond to the stages after adsorption of 2,4,6,8,10, and 12 alternate MB/PSS layers. Adapted from [10]

The assembly of glucose oxidase films (GOD/PEI) was reported by Lvov and co-workers [10]. The adsorption kinetics of this process yielded GOD adsorption saturation in 15 minutes. Linear film mass increases were observed up to at least 21 molecular layers. The layer thickness for GOD was 34.4nm and 0.8nm for PEI. In addition, with increasing numbers of GOD layers, a linear increase of the UV/Vis absorbance was observed [10].

The alternate assembly of glucose oxidase with PDDA was also reported [10,32]. Layer thicknesses observed with each adsorption cycle of GOD (8nm with PDDA; 11.7nm with PEI at pH 7; 8.4nm with PAA) correspond to the diameter of the GOD molecule, suggesting a monolayer formation [10,32].

Atomic Force Microscopy (AFM) has been used to study surface morphology of multilayered films at every step of the adsorption process [41]. Surface roughness corresponded to the sequence of protein/polyion adsorption. With the protein layer, the surface roughness was larger and corresponded to the diameter of the globular protein used. The surface roughness decreased upon the deposition of the polyion layer.

2.3 BIOLOGICAL ACTIVITY AND ENHANCED STABILITY OF PROTEINS IN FILMS

Proteins assembled with polyions by the layer-by-layer methodology tend to not denature [10,26,27,30,32,33,38]. The retention of enzymatic activities within the multilayered films was seen with glucose isomerase, glucoamylase, glucose oxidase, and peroxidase. Specific reactions was seen between immunoglobulins (IgG) and antibodies in the multilayered films [33]. The Soret band absorbance of myoglobin and hemoglobin was used to confirm their native conformations within the films [8,10,35]. Redox potentials of myoglobin and cytochrome P450 within those multilayered films corresponded to the redox potentials of these proteins immobilized onto electrode surfaces by other methods [35, 37].

Layer-by-layer immobilization of proteins with linear polyions enhanced their enzymatic stability, and preserved them from microbial attacks. GOD/PEI multilayered films retained 90% of enzymatic activity after incubation at 5°C for 3 months. In addition, GOD/PEI multilayered films show enhanced temperature stability and were active up to 67°C in comparison to 50°C for GOD in solution. Glucose oxidase retains its

activity within the multi-layered films up to pH 10 while it drops to a minimum at pH 9 in solution [32].

The enzymatic activity within the multilayered films increases linearly with the number of enzyme layers as seen with the GOD/PEI films up to 10 protein layers; when the activity of the film reaches saturation [32]. Saturation in bioactivity is probably due to diffusion limitations of the substrate in penetrating the film. The extent of accessibility of the substrate to the proteins within the film depends greatly on the nature of the film component, due to the transport of the substrate through the multilayer, and thus puts restrictions on the number of enzyme layers within the multilayered films.

2.4 PROBLEMS OF THE ASSEMBLY

2.4.1 NONLINEAR GROWTH

Nonlinear film growth with adsorption cycles was seen in some cases, and it was possible to overcome it in order to reach protein monolayer formation at every adsorption step by the following methods:

1. Decreasing of protein concentrations, such as in the case of pepsin/PDDA, or alcohol dehydrogenase/PDDA films, from 1mg/ml to 0.1mg/ml or less. IgG was also used for assemble at low concentrations (0.1mg/ml) [33].
2. Altering the pH of the protein solution in order to modulate the surface charge, as in the case of the GOD/PEI assembly from pH 6.5 to 9.2 [32].
3. Altering the types of polyions used in the layer-by-layer assembly procedure. In the case of GOD, monolayer formation was achieved via the change from branched PEI to linear PDDA [10], or PAA [32].

2.4.2 CHARGED GROUPS ON A PROTEIN GLOBULE SURFACE

Density and location of the charge

The density and location of the charge on the protein surface can be critical to the assembly process. The electrostatic attraction of proteins with linear polyions is straightforward, however, the situation is different with large ions with specific three-dimensional shapes and

charge distribution. As an example, the direct assembly of oppositely charged protein molecules was difficult due to the fact that electrostatic attractions cannot be maximized with globular proteins. Polyion anchoring appears to be favored by the "patched" nature of the surface charge of proteins [42]. Flexible linear polyions can produce optimized electrostatic attractions and hence may penetrate in between protein molecules acting as an electrostatic "glue".

The pH dependance

The number of excess charges on protein surfaces is directly dependant on the pH. Typically, the number of elemental charges seen with proteins used in the assembly process ranges from 10 to 60. For example, an albumin globule gave an elemental charge of +35 at pH 4 [31].

Dependence on the thickness of the underlying polyion layer

The amount of adsorbed proteins was found to depend on the thickness of the underlying linear polyion layer. Proteins deposited in alternation with polyions prepared from high ionic strength solutions

(thickness of polyion layer: 3-4nm) were thicker than the protein layers deposited in alternation with polyions prepared from water (thickness of polyion layer 1nm). In multilayers composed of myoglobin/PSS in 0.2M NaCl, the thickness of the myoglobin layer was of the order of 7nm, which is double the thickness of the 4nm myoglobin monolayer deposited in alternation with PSS from water [35]. The amount of immunoglobulins was found to be double in IgG/PSS in 0.1M NaCl multilayers when compared to a multilayer with PSS from water [33]. The thicker polyion layer provides a matrix with a greater area available for protein deposition, and hence requires more protein to achieve the charge compensation and reversal. Therefore, the variation in the ionic strength of the polyion solution may be used as a fine-tune properties of the protein surface in film buildup.

2.4.3 RELIEF OF SOLID SUPPORT

The stability of the multilayer assembly can be affected by the surface structure of the solid support. The assembly of hemoglobin, glucose oxidase, concanavalin, albumin, and myoglobin gave more stable films than those of cytochrome c and lysozyme. Multilayer assemblies

onto QCM resonator was successful on all those proteins, while some difficulties occurred with the assembly onto quartz slides such as in the case of the alternate assembly of lysozyme onto PSS. Protein multilayers exhibit high stability when deposited onto silver or gold electrode surfaces, which have roughness in the tens of nanometers range.

2.4.4 OTHER PROBLEMS

1) pH in the bulk of the solution might differ from the pH at the charged polyion surface which could influence the conformation and activity of proteins in addition to the interaction with the polyion layer itself.
2) The relative roughness of the polyion surface. Polymeric tails might protrude into the bulk solution causing protein aggregation during adsorption.
3) Drying of the polyion films might influence the structure.

2.5 CONCLUSIONS

This chapter gives an overall view of fundamental approaches developed to design organized protein films with precise location of different protein monolayers. The multilayer film formation utilizing the

layer-by-layer methodology may be applied to any water-soluble protein by choosing a solution pH apart from the protein isoelectric point to provide a surface charge. The films can be used in the following application areas:

1) Sensor layers. Multilayered films compromising enzymes layers provide a quick response to changes in its vicinity when combined with field-sensitive microelectronic elements. The efficiency of such sensor layers might be increased by the sequential deposition of the enzymatic layers that leads to enhanced electron transfer. Conductive polyions can be used to enhance electrical signaling processing as well. Protein/polyions multilayered films are insoluble in water and organic solvents and hence are perfectly suited for such uses.
2) Biocompatible coatings. Multilayered protein films may be used to coat surfaces of implants and surgical instruments. The use of functional proteins allows the preparation of biomimetic surfaces. In addition, polymer and polyion organic chemistry is extensive and hundreds of polyions may be used in the assembly with proteins. Mmultilayered films that result are molecularly thin and have

desirable architecture and composition. The multilayered protein films may cover any type of surfaces that carries a sufficient surface charge.

2.6 REFERENCES

1. Decher G, Hong JD. Buildup of Ultrathin Multilayer Films by a Self-Assembly Process .1. Consecutive Adsorption of Anionic and Cationic Bipolar Amphiphiles on Charged Surfaces. Makromolekulare Chemie-Macromolecular Symposia 1991;46:321-327.
2. Decher G. Fuzzy nanoassemblies: Toward layered polymeric multicomposites. Science 1997;277(5330):1232-1237.
3. Lvov Y, Decher G, Mohwald H. Assembly, Structural Characterization, and Thermal-Behavior of Layer-by-Layer Deposited Ultrathin Films of Poly(Vinyl Sulfate) and Poly(Allylamine). Langmuir 1993;9(2):481-486.
4. Lvov Y, Decher G, Sukhorukov G. Assembly of Thin-Films by Means of Successive Deposition of Alternate Layers of DNA and Poly(Allylamine). Macromolecules 1993;26(20):5396-5399.
5. Lvov Y, Haas H, Decher G, Mohwald H, Kalachev A. Assembly of Polyelectrolyte Molecular Films onto Plasma-Treated Glass. Journal of Physical Chemistry 1993;97(49):12835-12841.

6. Decher G, Essler F, Hong JD, Lowack K, Schmitt J, Lvov Y. Layer-by-Layer Adsorbed Films of Polyelectrolytes, Proteins or DNA. Abstracts of Papers of the American Chemical Society 1993;205:334-Poly.
7. Decher G, Lvov Y, Schmitt J. Proof of Multilayer Structural Organization in Self-Assembled Polycation Polyanion Molecular Films. Thin Solid Films 1994;244(1-2):772-777.
8. Lvov Y, Ariga K, Kunitake T. Layer-by-Layer Assembly of Alternate Protein Polyion Ultrathin Films. Chemistry Letters 1994(12):2323-2326.
9. Lvov Y, Haas H, Decher G, Mohwald H, Mikhailov A, Mtchedlishvily B, et al. Successive Deposition of Alternate Layers of Polyelectrolytes and a Charged Virus. Langmuir 1994;10(11):4232-4236.
10. Lvov Y, Ariga K, Ichinose I, Kunitake T. Assembly of Multicomponent Protein Films by Means of Electrostatic Layer-by-Layer Adsorption. Journal of the American Chemical Society 1995;117(22):6117-6123.

11. Mendelsohn JD, Yang SY, Hiller J, Hochbaum AI, Rubner MF. Rational design of cytophilic and cytophobic polyelectrolyte multilayer thin films. Biomacromolecules 2003;4(1):96-106.
12. Elbert DL, Herbert CB, Hubbell JA. Thin Polymer Layers Formed by Polyelectrolyte Multilayer Techniques on Biological Surfaces. Langmuir 1999;15(16):5355-5362.
13. Schlenoff JB, Dubas ST, Farhat T. Sprayed Polyelectrolyte Multilayers. Langmuir 2000;16(26):9968-9969.
14. Ai H, Jones SA, Lvov YM. Biomedical applications of electrostatic layer-by-layer nano-assembly of polymers, enzymes, and nanoparticles. Cell Biochem Biophys 2003;39(1):23-43.
15. Smuleac V, Butterfield DA, Bhattacharyya D. Layer-by-layer-assembled microfiltration membranes for biomolecule immobilization and enzymatic catalysis. Langmuir 2006;22(24):10118-10124.
16. Lvov Y. Electrostatic layer-by-layer assembly of proteins and polyions. In: Lvov Y, and Mohwald, H.M., editor. Protein Architecture: Interfacing Molecular Assemblies and Immobilization Biotechnology. New York: Dekker; 2000. p. 125-167.
17. Serizawa T, Yamaguchi M, Akashi M. Alternating bioactivity of polymeric layer-by-layer assemblies: Anticoagulation vs

procoagulation of human blood. Biomacromolecules 2002;3(4):724-731.

18. Koga J, Yamaguchi K, Gondo S. Immobilization of Alkaline-Phosphatase on Activated Alumina Particles. Biotechnology and Bioengineering 1984;26(1):100-103.

19. Bhatia RB, Brinker CJ, Gupta AK, Singh AK. Aqueous sol-gel process for protein encapsulation. Chemistry of Materials 2000;12(8):2434-2441.

20. Li ZF, Kang ET, Neoh KG, Tan KL. Covalent immobilization of glucose oxidase on the surface of polyaniline films graft copolymerized with acrylic acid. Biomaterials 1998;19(1-3):45-53.

21. Godjevargova T, Konsulov V, Dimov A, Vasileva N. Behavior of glucose oxidase immobilized on ultrafiltration membranes obtained by copolymerizing acrylonitrile and N-vinylimidazol. Journal of Membrane Science 2000;172(1-2):279-285.

22. Vishwanath SK, Watson CR, Huang W, Bachas LG, Bhattacharyya D. Kinetics studies of site-specifically and randomly immobilized alkaline phosphatase on functionalized membranes. Journal of Chemical Technology and Biotechnology 1997;68(3):294-302.

23. Ganapathi-Desai S, Butterfield DA, Bhattacharyya D. Kinetics and active fraction determination of a protease enzyme immobilized on functionalized membranes: Mathematical modeling and experimental results. Biotechnology Progress 1998;14(6):865-873.

24. Butterfield DA, Bhattacharyya D, Daunert S, Bachas L. Catalytic biofunctional membranes containing site-specifically immobilized enzyme arrays: a review. Journal of Membrane Science 2001;181(1):29-37.

25. Keller SW, Kim H-N, Mallouk TE. Layer-by-Layer Assembly of Intercalation Compounds and Heterostructures on Surfaces: Toward Molecular "Beaker" Epitaxy. J. Am. Chem. Soc. 1994;116(19):8817-8818.

26. Kong W, Zhang X, Gao ML, Zhou H, Li W, Shen JC. A New Kind of Immobilized Enzyme Multilayer Based on Cationic and Anionic Interaction (Vol 15, Pg 405, 1994). Macromolecular Rapid Communications 1994;15(10):805-805.

27. Kong W, Wang LP, Gao ML, Zhou H, Zhang X, Li W, et al. Immobilized Bilayer Glucose-Isomerase in Porous Trimethylamine Polystyrene-Based on Molecular Deposition. Journal of the Chemical Society-Chemical Communications 1994(11):1297-1298.

28. Pommersheim R, Schrezenmeir J, Vogt W. Immobilization of Enzymes by Multilayer Microcapsules. Macromolecular Chemistry and Physics 1994;195(5):1557-1567.
29. Lvov Y, Ariga K, Ichinose I, Kunitake T. Layer-by-Layer Architectures of Concanavalin a by Means of Electrostatic and Biospecific Interactions. Journal of the Chemical Society-Chemical Communications 1995(22):2313-2314.
30. Onda M, Lvov Y, Ariga K, Kunitake T. Sequential reaction and product separation on molecular films of glucoamylase and glucose oxidase assembled on an ultrafilter. Journal of Fermentation and Bioengineering 1996;82(5):502-506.
31. Houska M, Brynda E. Interactions of proteins with polyelectrolytes at solid/liquid interfaces: Sequential adsorption of albumin and heparin. Journal of Colloid and Interface Science 1997;188(2):243-250.
32. Hodak J, Etchenique R, Calvo EJ, Singhal K, Bartlett PN. Layer-by-layer self-assembly of glucose oxidase with a poly(allylamine)ferrocene redox mediator. Langmuir 1997;13(10):2708-2716.

33. Caruso F, Niikura K, Furlong DN, Okahata Y. Assembly of alternating polyelectrolyte and protein multilayer films for immunosensing .2. Langmuir 1997;13(13):3427-3433.
34. Caruso F, Lichtenfeld H, Giersig M, Mohwald H. Electrostatic self-assembly of silica nanoparticle - Polyelectrolyte multilayers on polystyrene latex particles. Journal of the American Chemical Society 1998;120(33):8523-8524.
35. Lvov YM, Lu Z, Schenkman JB, Zu X, Rusling JF. Direct Electrochemistry of Myoglobin and Cytochrome P450cam in Alternate Layer-by-Layer Films with DNA and Other Polyions. J. Am. Chem. Soc. 1998;120(17):4073-4080.
36. He JA, Samuelson L, Li L, Kumar J, Tripathy SK. Oriented bacteriorhodopsin/polycation multilayers by electrostatic layer-by-layer assembly. Langmuir 1998;14(7):1674-1679.
37. Kong J, Lu Z, Lvov YM, Desamero RZB, Frank HA, Rusling JF. Direct Electrochemistry of Cofactor Redox Sites in a Bacterial Photosynthetic Reaction Center Protein. J. Am. Chem. Soc. 1998;120(29):7371-7372.
38. Onda M, Lvov Y, Ariga K, Kunitake T. Sequential actions of glucose oxidase and peroxidase in molecular films assembled by layer-by-

layer alternate adsorption. Biotechnology and Bioengineering 1996;51(2):163-167.

39. Caruso F, Furlong DN, Ariga K, Ichinose I, Kunitake T. Characterization of polyelectrolyte-protein multilayer films by atomic force microscopy, scanning electron microscopy, and Fourier transform infrared reflection-absorption spectroscopy. Langmuir 1998;14(16):4559-4565.

40. Lvov Y, Ariga K, Ichinose I, Kunitake T. Molecular film assembly via layer-by-layer adsorption of oppositely charged macromolecules (linear polymer, protein and clay) and concanavalin A and glycogen. Thin Solid Films 1996;285:797-801.

41. Onda M, Lvov Y, Ariga K, Kunitake T. Molecularly flat films of linear polyions and proteins obtained by the alternate adsorption method. Japanese Journal of Applied Physics Part 2-Letters 1997;36(12A):L1608-L1611.

42. Park JM, Muhoberac BB, Dubin PL, Xia J. Effects of protein charge heterogeneity in protein-polyelectrolyte complexation. Macromolecules 1992;25(1):290-295.

CHAPTER III

NITRIC OXIDE SYNTHASE OXYGENASE BASED NITRIC OXIDE RELEASE POLYETHYLENEIMINE THIN FILMS

3.1 INTRODUCTION

Graft thrombosis is the cause of 80% of vascular access dysfunction, a problem with an associated health-care cost of over $1 billion/year [1]. The number of revascularization procedures have increased dramatically, and is estimated at 15% after initial coronary revascularization, and approximately 50% after lower extremity bypass [2, 3]. Stent restenosis occurs at 30% of implant sites as a result of initial vascular thrombosis followed by cell proliferation, requiring a repeat angioplasty procedure within 1 year [4].

The thrombogenic nature of various polymeric materials utilized to prepare blood-contacting and implantable medical devices such as vascular grafts, intravascular catheters, sensors, coronary artery and vascular stents, and a host of other medical tools, even if labeled as biocompatible, can cause serious complications in patients. Thrombus formation at the surface of implantable medical devices is the major cause of vascular access dysfunction requiring secondary vascular procedures. Upon introduction of a foreign material into the blood stream, key proteins of the coagulation cascade (fibrinogen, and von Willebrand's factor) adsorb on the surface, followed by platelet adhesion and activation, leading to fibrin and thrombus formation at the surface (Figure 3.1).

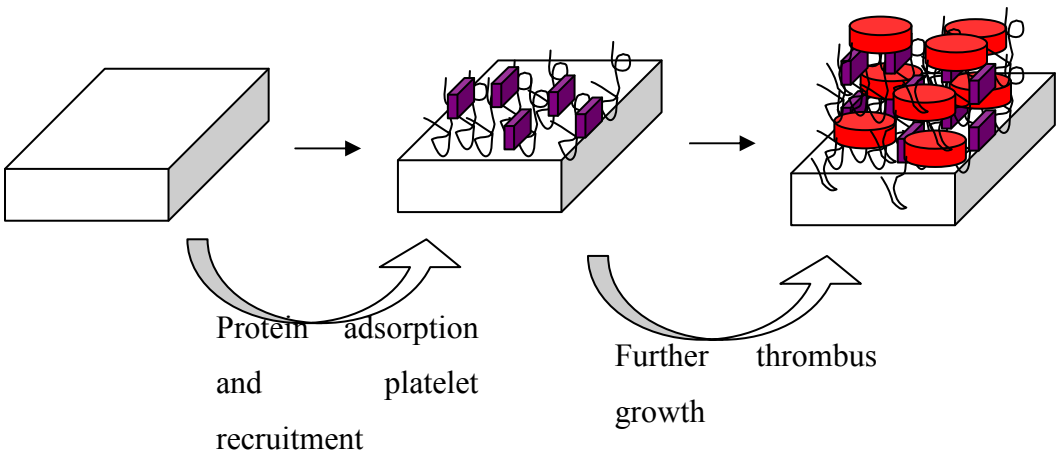

Figure 3.1: Illustration showing thrombus formation at the surface of implantable medical devices. Upon exposure to blood, protein adsorption occurs, followed by platelet adhesion at the surface. Platelet activation leads to thrombus formation at the surface.

An anti-coagulation regiment, with the adverse effects associated with long term use, is typically required to clinically reduce the risk of thrombus formation [5]. Thrombus formation involves two synergistic events; a cGMP-dependant mechanism that involves platelet activation, adhesion and aggregation [6], and fibrin formation resulting from the binding of bivalent fibrinogen to glycoprotein IIb/IIIa [7].

Nitric oxide (NO), a molecule generated by the enzyme Nitric Oxide Synthase [8], using L-arginine as a substrate, was recently identified as a potent antiplatelet agent. This small molecule orchestrates a myriad of vital physiological functions. For instance, the endothelium-derived NO production at low concentrations (nanomolar) plays a critical role in the regulation of vascular hemostasis [9], and inhibits platelet adhesion [10], and aggregation [11], as well as their further recruitment to the growing thrombus [12]. There have been numerous reports indicating NO release from resting [13] and aggregating platelets [14]. NO flux from activated human platelets have been indirectly measured and is estimated at ~1.2 $pmol.min^{-1}/10^{8}$ cells [13]. NO temporarily inactivates platelets in the close proximity of the endothelium [15]. This inhibition is short-lived and NO is rapidly scavenged by oxygen and hemoglobin in plasma [16]. To maintain this vital function and

counteract thrombus formation, stimulated human endothelial cells continuously generate NO at a level of *ca.* $4x10^{-10}$ $mol.cm^{-2}$ min^{-1} [17]. In this regard, NO-releasing bio-polymers are targeted as effective anti-thrombotic coatings in an attempt to enhance thromboresistivity of blood-contacting medical devices and implants.

Numerous approaches are investigated in an attempt to develop polymeric materials that are more blood-compatible. In general, these approaches can be categorized into two main trends: first, methods that mimic the anti-thrombogenic properties of endothelial cells [18], and, second, methods that use modified chemical surfaces and added moieties that limit protein and cell adhesion [19]. Prevention of protein adhesion *in vivo* is generally difficult to achieve, therefore the other approach, which aims at the development of surfaces mimicking properties of native endothelial cells, appears more promising. Nitric oxide, thrombomodulin, prostacyclin, and heparans contribute to the non-thrombogenic properties of the endothelial cells [20]. A potential solution can be found in polymeric coating materials that are capable of releasing low levels of nitric oxide at the blood/coating interface. Considerable efforts in this research area are focused on improving the NO-release chemistry of materials used as outer coatings for implantable medical

devices. Polymers that possess chemical platforms with the ability of releasing NO have been shown to exhibit varying levels of thromboresistivity. In fact, akin to nitric oxide-releasing endothelial cells, NO-releasing polymers as functional coatings have the potential to be effective in preventing platelet adhesion, activation, and aggregation onto surfaces. These coatings have the potential of reducing the risk of thrombus formation at the exterior of blood-contacting devices and implants. They also have the potential to prolong vascular graft and stent potency without adverse systemic effects [21].

Two classes of NO-releasing materials have been explored. N-diazeniumdiolate based NO-releasing polymers [22], and Nitrosothiol-based NO-releasing polymers [23]. N-diazeniumdiolates are inorganic NO donors formed by the reaction of a secondary amine structure with 2 equivalents of NO gas under high pressure, creating a relatively stable adduct structure [24]. The general structural types of diazeniumdiolates used for NO-releasing polymers include dispersed non covalently bound small molecules where the diazeniumdiolate group is attached to amines in low molecular weight compounds, and covalently bound diazeniumdiolates group to polymeric side chains or to the polymeric backbone [22].

The second class of proposed NO donors are S-nitrosothiols [25]; they mimic biological systems that are thought to serve as a NO reservoirs and transporters, such as S-nitroso-albumin and S-nitrosoglutathione, which are the most abundant naturally occurring S-nitrosothiols circulating in blood [26].

While films made of NO-donors incorporated into polymeric matrices did show the functional worthiness of NO-releasing coatings, this approach naturally results in only finite NO reservoirs, and thus the corresponding coatings are limited in their ability to sustain antithrombotic function over prolonged periods of time. The finite NO reservoir approach will also limit the potential use in more permanent types of implants. In addition, the NO fluxes achieved so far are lower than NO released from endothelial cells [19]. The logical alternative is then to explore approaches that would lead to materials with the ability to sustain NO generation for longer durations and at levels comparable to stimulated human endothelial cells (*ca.* $4x10^{-10}$ $molcm^{-2}min^{-1}$) [17] and/or potentially tunable levels.

Developing NO-releasing surfaces that closely resembles the endothelium is critical to achieving better thromboresistivity. The endothelial isoform of the enzyme nitric oxide synthase, eNOS, is a key

component of the endothelial cell lining. It was reported that eNOS-overexpressing endothelial cells seeding of synthetic small diameter vascular grafts decreased human platelet aggregation by 46%, and bovine aortic smooth muscle cell proliferation by 67.2% *in vitro* [27]. NO-releasing materials using polyethyeleneimine (PEI), a biocompatible polymer [28], has been reported in literature [29]. In our lab, NO was successfully generated from the enzyme nitric oxide synthase embedded in bilayered cast surfactant films [30].

In this work, we incorporated the enzyme nitric oxide synthase in the PEI polymeric matrix by means of layer-by-layer electrostatic adsorption [8], to construct a multicomponent protein film that mimics the NO-generating behavior of the endothelial cell lining. We demonstrate in this paper that our films provide a viable source of NO that utilizes endogenous compounds to maintain a continuous supply of nitric oxide. This study is the first account of successful NO release from the enzyme nitric oxide synthase incorporated into a bio-polymeric matrix using a LBL assembly technique. Our NO-releasing biopolymer coating is successfully formed by alternate deposition of polyethyleneimine and NO-generating NOS enzymes.

3.2 RESULTS AND DISCUSSION

3.2.1 EXPRESSION AND PURIFICATION OF iNOSoxy VIA RECOMBINANT PLASMID DNA

Many proteins and enzymes can be purchased through chemical catalogs with moderate expense making them best procured through those sources. NOS is not one of them. Because of the small biological quantities found in animal tissue, preparation and purification from biological sources would be prohibitively expensive. Making the procurement even more prohibitive is the fact that we need to specifically target the oxygenase domain of the enzyme, which could be obtained separate from the reductase domain by limited proteolysis of the full-length strand. However, to use NOS enzyme in the quantities required for the completion of the current study requires an unbroken, relatively inexpensive source of enzyme without the tedious extra steps involved with enzyme proteolysis. This is accomplished through in-house protein expression and purification of the oxygenase domain via recombinant plasmid DNA.

The pCWori vector, a generous gift from the laboratory of Dennis Stuehr at the Lerner Research Institute, is inserted into plasmid DNA and transformed into BL21 (DE3) ampicillin-resistant *E. coli* as detailed by the Stuehr group [31]. This glycerol stock is then inoculated into 2 x 2 ml LB medium with 100 μg/ml added ampicillin and allowed to grow overnight at 37^{o}C.

Each aliquot of overnight culture is added to 500 ml autoclaved TB solution and allowed to grow under agitation at 37°C for about 3 hours or until 0.1 OD_{600} is reached. Temperature is dropped to 25°C until 0.3 – 0.8 OD_{600} is reached, at which time IPTG and δ-aminolevulinic acid are added to induce iNOSoxy protein production and to provide a heme precursor for the metalloprotein. The induced culture is left again overnight to produce maximum quantities of protein. Cells are harvested by centrifugation at 4,000 rpm at 4°C for 30 minutes, drained of supernate, and resuspended in a minimum of pH 7.6 lysis buffer containing base buffer, lysozyme, phenylmethanesulfonylfluoride (PMSF), Protease Inhibitor III (4-(2-Aminoethyl) benzenesulfonyl fluoride hydrochloride, aprotinin, leupetin, pepstatin A, bestatin, and L-3-trans-Carboxyoxiran-2-carbonyl)-L-leucyl-agmatin), DNase, and $MgCl_2$. Cells are lysed by sonication at 15-second on, 45-second off intervals for

a period of twenty minutes. The sonicated suspension is centrifugated at 12,000 g at 4°C for 30 minutes to precipitate cellular debris. The debris pellet is discarded and the crude supernatant lysate is collected. Protein precipitation is induced by gradual addition of 0.300 g $(NH_4)_2SO_4$/ml of solution over a period of 1 hour followed by centrifugation at 10,000 rpm to collect the protein pellet. The pellet is again resuspended in base buffer, PMSF, and Protease Inhibitor III and filtered through a 0.45 micron PES syringe filter. A 4 ml dead volume Ni-NTA Agarose column is prepared for use by charging with 50 mM $NiSO_4$, followed by addition of a binding tris buffer before loading the filtered protein sample onto the column. The column is equilibrated with tris binding buffer and washed with a dilute (40 mM) imidazole wash buffer prior to elution with c. 200 mM imidazole elution buffer. The protein was collected off the column and dialyzed in 500 ml base buffer with 200 µl β-mercaptoethanol, changing dialysis solution twice during the overnight process. The dialyzed protein is further concentrated by centrifugation at 5000 rpm at 4°C using 30,000 MW cut-off Amicon filters until the desired concentration (usually 0.45 mM) is reached. Aliquots of the protein are stored at -80°C for future use. Protein concentration is determined by Bradford Assay and by UV-Vis analysis of the Soret band

at 421 nm. SDS-PAGE further confirms the presence of iNOSoxy by marker comparison to molecular weight standards.

3.2.2 PREPARATION OF PEI/NOSoxy FILM

We report here a proof of principle with the NOS oxygenase domain. The tetrahydrobiopterin-free oxygenase domain of inducible nitric oxide synthase (iNOSoxy) was expressed in house as reported in literature [32], and was used to explore the viability of nitric oxide synthase-containing films as potential sources of nitric oxide release. Although other surfaces can be used for film formation, we describe here the example of conductive pyrolytic graphite as a surface in order to perform, in parallel, the electrochemical characterization of nitric oxide synthase enzyme embedded in the polymetric film, as will be described later. The pyrolytic graphite surface is initially chemically oxidized as described in the literature to obtain a uniform negative charge at the surface [33]. The negatively-charge surface is then alternatively dip-coated in polyethyleneimine (1.5 mg/ml) solution and iNOSoxy (20 mg/ml) solution for 20 minutes, respectively, to achieve the desired film composition of 3 layers of iNOSoxy embedded in 4 alternate layers of

PEI unless stated otherwise. The surface is thoroughly washed with deionized water and air-dried after each dip-coating step. The films were stored overnight at 4°C. (Figure 3.2)

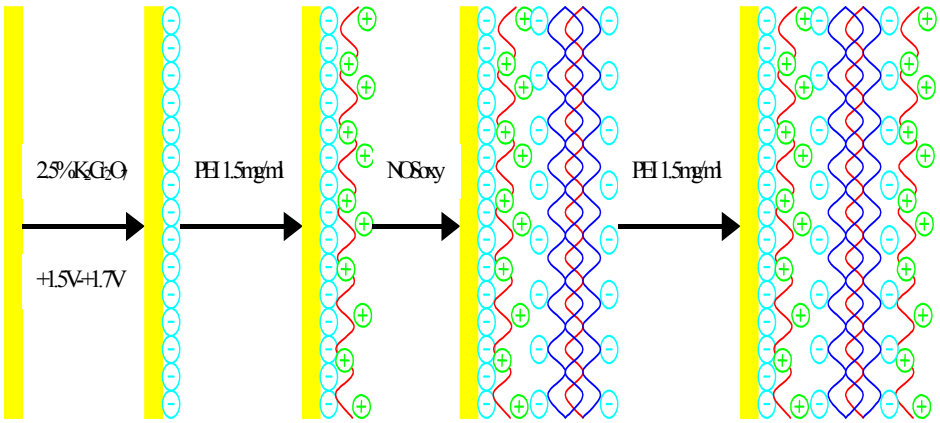

Figure 3.2: Assembly of PEI/NOSoxy film using layer-by-layer electrostatic deposition.

3.2.3 FT-IR SPECTROSCOPIC CHARACTERIZATION

We first performed IR characterization of the iNOSoxy in PEI films. Figure 3.3 shows the IR spectrum of iNOSoxy sandwished in layers of PEI. The spectrum is focused in the amide-1 and amide-2 IR region, which is often used to probe structural changes in globular proteins. Figure 1 shows that the overall shapes and positions of the two amide-bands are conserved in PEI films compared to native iNOSoxy in the absence of PEI. This result shows that the iNOSoxy conserves its major globular structure features in the PEI thin film.

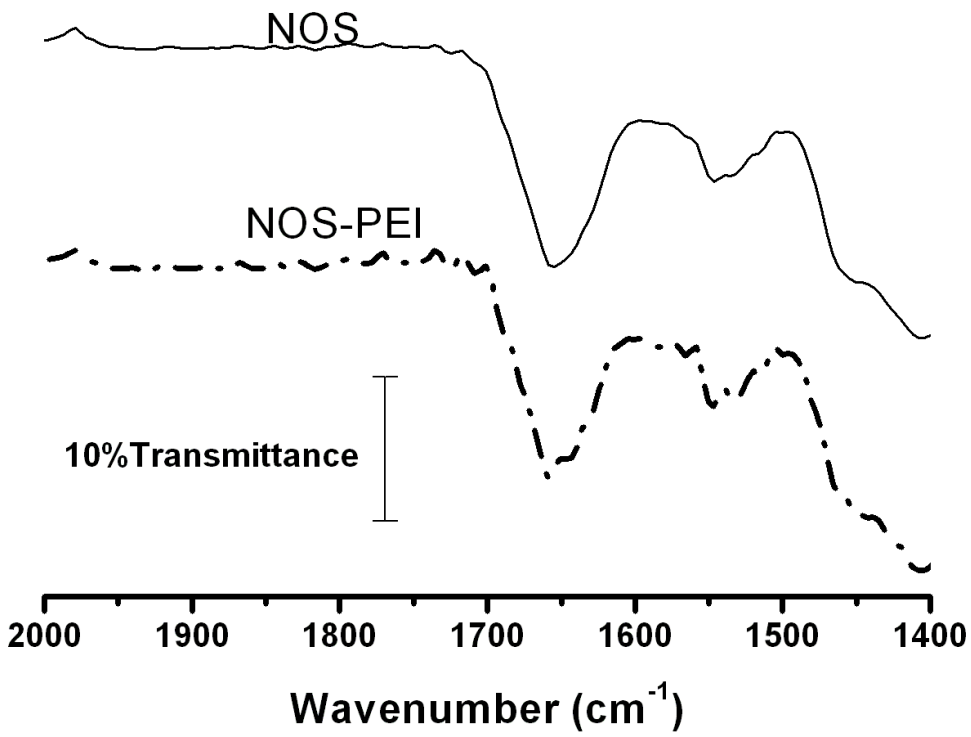

Figure 3.3: Infrared spectrum in the amide I and amide II IR region showing that these bands, as spectroscopic probes of the NOSoxy structure in the PEI film, are conserved.

3.2.4 ELECTROCHEMICAL CHARACTERIZATION

To characterize the functional integrity of iNOSoxy embedded in the PEI film, we examined the electrochemical reduction of NO by iNOSoxy in film at the surface of pyrolytic graphite electrodes. The experiments for the characterization of NOS functional integrity using NO are carried out in the absence of oxygen. For these experiments only, the buffer is typically purged with purified nitrogen for at least 30 min prior to the experiments. A nitrogen blanket was then kept over the solution throughout the experiments. A fresh solution of 2mM NO was prepared, and required aliquots are added to the solution to make the desired concentration increments. NO stock-solutions are made by bubbling pure NO gas through degassed water [34]. NOSoxy enzymes, like other heme proteins and P-450 enzymes, can catalyze the electrochemical reduction of the nitric oxide as a substrate [35, 36]. We used this known property to characterize the presence and function of iNOSoxy enzymes embedded between the PEI layers in our thin films. Cyclic voltammetry of PEI/iNOSoxy film at the surface of PG electrodes (Figure 3.4) illustrates an irreversible catalytic wave at –0.9V/s, a

response typical to the catalytic reduction of NO by a heme protein such as iNOSoxy [35, 36].

A negative control experiment (PEI film devoid of iNOSoxy), does not show a catalytic current at –0.9V/s at the same NO concentrations (Figure 3.5). The increase in catalytic currents at –0.9V/s upon incremental additions of NO is a clear indication of iNOSoxy catalytic mediation, and further confirms that its structural integrity and catalytic function are preserved in the in our PEI films. The native structure and integrity of embedded NOS enzyme and related enzymatic function are critical to the successful fabrication of our targeted NOS-based NO-releasing films.

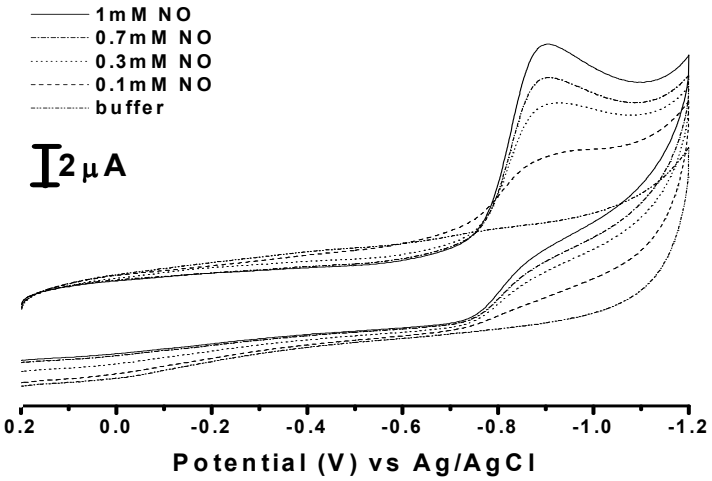

Figure 3.4: Cyclic voltammograms of catalytic reductions of NO by PEI/NOS films at the surface of a PG electrode in pH 7.0 for different NO concentrations. The film on the electrode was formed by the alternate deposition of 5 layers of NOS enzyme sandwiched between PEI layers.

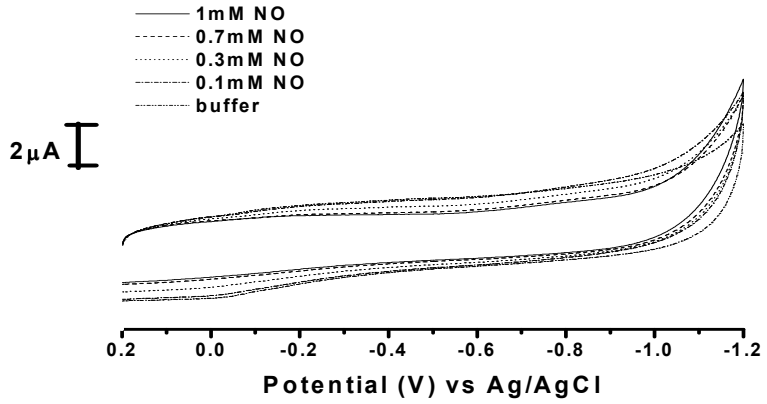

Figure 3.5: Negative control showing no catalytic reduction of NO on PEI films devoid of iNOSoxy protein

3.2.5 ATOMIC FORCE MICROSCOPY

To investigate the success of our methodology in producing polymeric film coatings with the desired coverage and surface morphology, we further characterized our LBL deposition of film components using atomic force microscopy (AFM) imaging. Figure 3.6 illustrates the AFM image of the layer-by-layer iNOSoxy/PEI film buildup. Figure 3.6A shows the 3D AFM image of the deposition of a layer of iNOSoxy over a layer of the polymer PEI at the surface of the HOPG slide. The figure shows a uniform distribution of the enzyme over the surface. Closer analysis of the features that result upon exposure to iNOSoxy solution confirms that the observed dimensions are close to the crystallographic dimension of iNOSoxy [37]. The overall surface height is of the order of 70 Å. Figure 3.6B shows the AFM image of the same HOPG slide after the sequential deposition of PEI over a layer of iNOSoxy resulting in the PEI/iNOSoxy/PEI coating. This image shows that the layer of iNOSoxy is still present but is now embedded in between two alternate PEI layers. The biocompatible polymeric coat now brings the average surface height to the order of 80 Å, which is consistent

with the cumulative surface heights measured for the PEI layers an the layer of iNOSoxy.

Our step-by-step AFM characterization shows that the functional component of our films, i.e. the iNOSoxy enzyme, is successfully trapped in between layers of the PEI polymer. In addition, AFM imaging shows that our LBL methodology yields a thin film with uniform coverage of the surface. A uniform coverage of the surface is key for efficiently prohibiting seed contacts at the blood/device interface, which will help improve the thromboresistivity of the device.

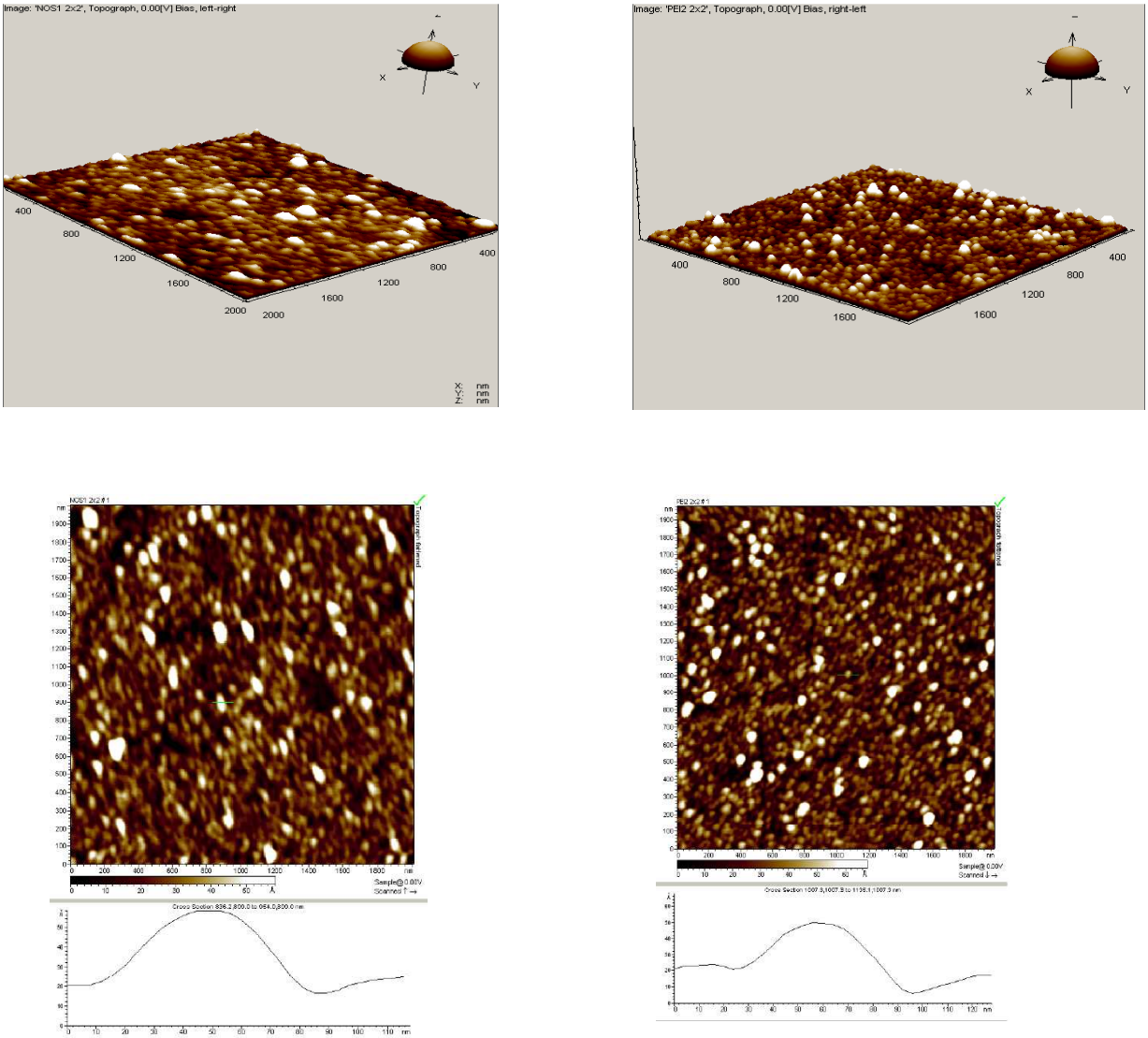

Figure 3.6: Atomic force microscopy images at the surface of highly oriented pyrolytic graphite (HOPG) depicting typical PEI/NOS film composition. (A) is a 2µmx2µm 3D scan of a layer of NOS enzyme deposited over a layer of PEI polymer. (B) is µmx2µm 3D scan of the final layer of PEI polymer deposited after the deposition of a NOS enzyme layer.

3.2.6 QUARTZ CRYSTAL MICROBALANCE (QCM) CHARACTERIZATION

Quartz Crystal Microbalance (QCM) was used as a tool to investigate mass changes upon the alternate deposition of PEI and the NOSoxy enzyme. QCM analysis was carried out at the surface of a thin oscillating quartz crystal sandwiched between two gold electrodes. The measurement of the resonant frequency changes at the surface of a modified quartz crystal with the alternate deposition of PEI and iNOSoxy at the surface of a quartz crystal indicates a decrease in frequency that correlates with mass increase at the surface. Figure 3.7A indicates a typical QCM plot of the frequency change ΔF_0 upon the alternate deposition of PEI and the NOS enzyme on a quartz crystal. The average change in frequency per layer deposited is ΔF_0= 120 Hz as indicated by Figure 3.7A.

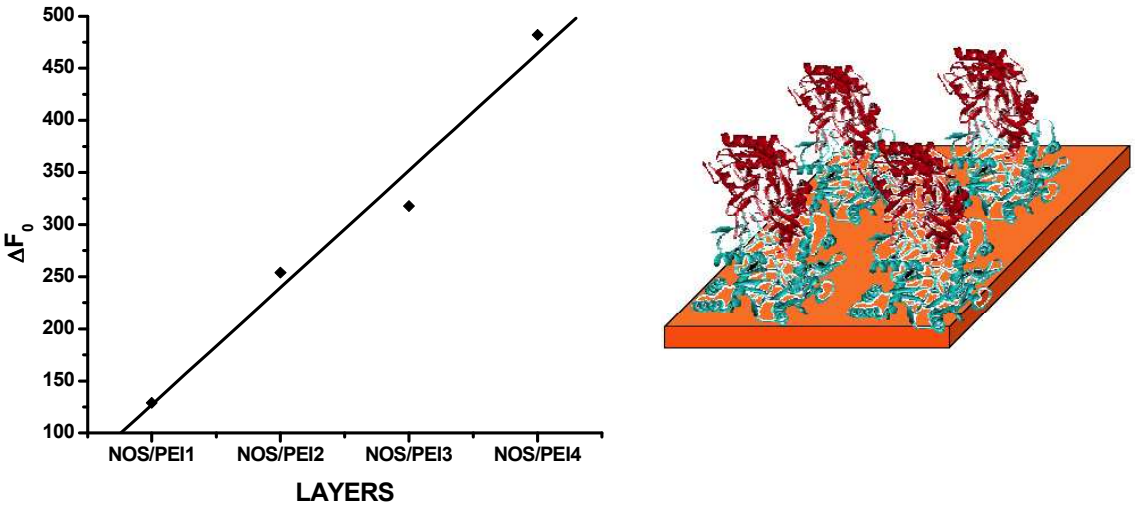

Figure 3.7: A- Monitoring of the PEI/NOS multilayer film building through the layer-by-layer methodology using quartz crystal microbalance. B- Proposed model based on measured changes in crystal frequency showing that iNOSoxy in a monolayer of double-stack (vertical) dimers in each layer of iNOSoxy in the LBL process.

The change in frequency can be converted to mass changes by the Sauerbrey equation [38]. The mass change obtained in addition to the known dimensions of the iNOSoxy enzyme (60x50x40 Å), and the molecular weight of the iNOSoxy (60kDa) allows the determination of a model of the enzyme orientation within the PEI film. A monolayer of double-stacked iNOSoxy dimers (as seen in Figure 3.7B) corresponds to a theoretical ΔF_0= 118 Hz which is of the same magnitude as the ΔF_0 seen experimentally. iNOSoxy is catalytically active in the dimeric form hence indicating that the charge-dependant orientation of the enzyme within the PEI matrix is such to retain its function.

3.2.7 NITRIC OXIDE FLUX MEASUREMENTS

Successful NO release was achieved from our PEI/NOS films and at fluxes higher than what have been reported in the literature for other inorganic NO-releasing systems [19]. Typical substrates prepared as described above are utilized to investigate the NO production capability from the trapped iNOSoxy enzymes. For the flux measurement of NO released from the NOS/PEI films, we used a reaction cocktail composed of the intermediate N-hydroxy-L-arginine (NHA; 100μM) [39],

tethrahydrobiopterin (H_4B; 10μM), Dithiothreitol (DTT; 400μM) in phosphate buffer (100mM; pH=7.4). Hydrogen peroxide (H_2O_2) was used as a source of reducing equivalents in the known NOS peroxide shunt reaction. The enzymatic reaction was run at 37°C for the desired time period. The enzymatic activity of the PEI/NOS film was quantified by measuring NO released using the Griess assay [40] which tracks the accumulation of nitrite as the decomposition product of NO generated by iNOSoxy in the film. Figure 3.8 reveals total NO release from films composed of 3 consecutive layers of PEI/NOS. An increase in NO released is achieved with increasing time.

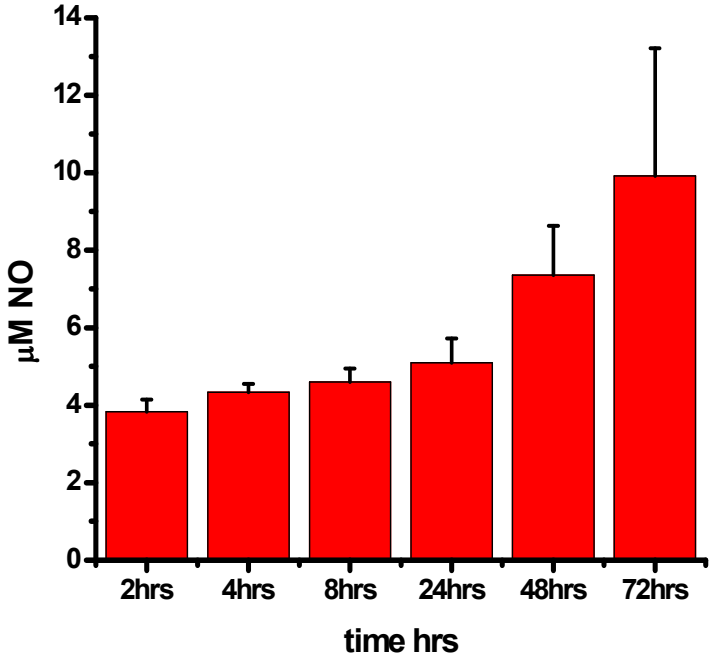

Figure 3.8: Total surface NO flux from PEI/NOS preparation as determined by the Griess assay. The PEI/NOS film is composed of 3 layers of NOS enzyme sandwiched between alternate PEI polymer layers. n=6

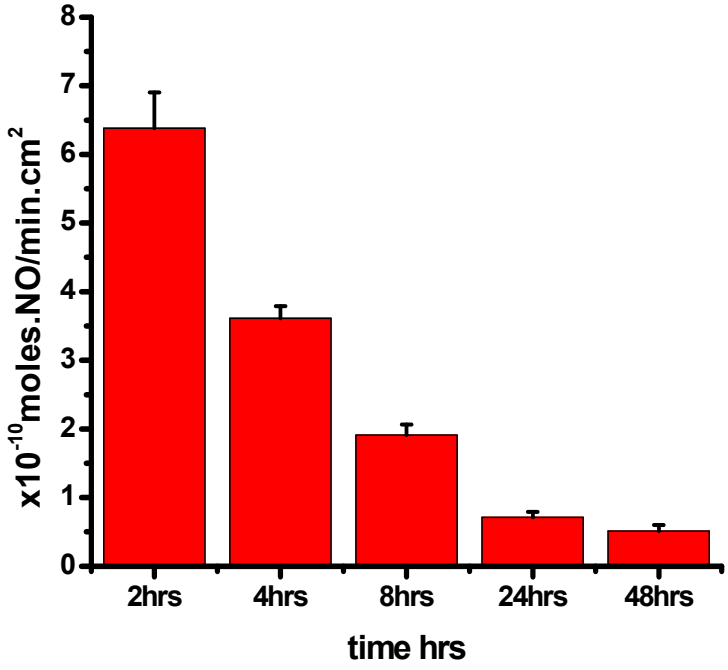

Figure 3.9: NO surface flux vs time from PEI/NOS preparation as determined by the Griess assay. The PEI/NOS film is composed of 3 layers of NOS enzyme sandwiched between alternate PEI polymer layers. n=6

Figure 3.9 shows the cumulative NO production by the (PEI/iNOSoxy) coating in terms of normalized NO surface flux. The figure shows that an initial burst of NO occurs at ~2 hours ($6.377x10^{-10}$ moles $NO.min^{-1}.cm^{-2}$ ± 0.523; n=6), 4 hours ($3.611x10^{-10}$ moles $NO.min^{-1}.cm^{-2}$ ± 0.177; n=6), 8 hours ($1.913x10^{-10}$ moles $NO.min^{-1}.cm^{-2}$ ± 0.148; n=6), followed by a sustained release at 24 hours ($0.707x10^{-10}$ moles $NO.min^{-1}.cm^{-2}$ ± 0.08; n=6), and 48 hours ($0.511x10^{-10}$ moles $NO.min^{-1}.cm^{-2}$ ± 0.088; n=6). Successful NO release was achieved from our PEI/NOS films and at fluxes higher than what have been reported in the literature for other inorganic NO-releasing systems.[19] Our PEI/iNOSoxy film sustained catalytic production of NO for long periods of time and in conditions that mimic physiologic settings. This proof of concept based on using NOS oxygenase domain shows that the enzyme, although trapped in the polymeric matrix, is still accessible by the N-hydroxy-L-arginine as a substrate surrogate and hydrogen peroxide as a source of electrons in solution. Nitric oxide is produced as a result of the NOSoxy-mediated catalytic oxidation of N-hydroxy-L-arginine. Our enzyme-based NO production approach in the biocompatible PEI film closely mimics the behavior of endothelial cells and essentially overcomes the shortcoming of other approaches that result in only finite

NO-reservoirs. Sustained NO fluxes were observed for a period of 72 hours. NO fluxes at 2 hours ($6.377x10^{-10}$ molesNO.min^{-1}.cm^{-2}) are 150 fold higher than fluxes from stimulated human endothelial cells ($4x10^{-10}$ mol.min^{-1}.cm^{-2}).[17] This initial burst eventually settles down at longer periods. For instance, the average NO flux at 48 hours is around only ($0.511x10^{-10}$ molesNO.min^{-1}.cm^{-2}), a value that is still ten-fold higher than NO fluxes from stimulated human endothelial cells. In addition, they are over 1000-fold higher than NO released from platelets.[13] NO release from PEI films shows 2-phase kinetics: an initial burst of NO, followed by a sustained release over a longer period of time. This 2-phase kinetics of NO release is in line with previously published studies.[41] The initial burst can be useful to counter early prosthetic graft occlusion that occurs in 18% of synthetic vascular access conduits for dialysis [42], and 25% of infrapoliteal synthetic grafts.[3] The PEI/NOS film has the ability to function as a thromboresistant scaffold that imitates the endothelial cell lining response through the biphasic NO release exhibited.

To monitor the effects of film thickness on NO fluxes we investigated NO release from films with varying numbers of iNOSoxy layers. Figure 3.10 shows increased NO fluxes from a film composed of

5 layers of PEI/NOS relative to a film preparation of 3 layers of PEI/NOS, indicating that higher NO fluxes can be achieved by increasing the thickness, i.e. enzyme loading, of the polymeric coatings. The rate of NO release is crucial, and the optimum NO levels for coatings to be applied on medical devices and blood-contacting implants are yet to be determined. Therefore, the ability to control NO fluxes is of utmost importance. Our layer-by-layer approach provides the ability to control NO fluxes from films by varying the number of NOS enzyme layers in the polymeric matrix. In addition to producing nanometer-thick coatings, the layer-by-layer electrostatic self-assembly method has the built-in ability to tweak the film architecture to meet the requirements of thickness and composition.

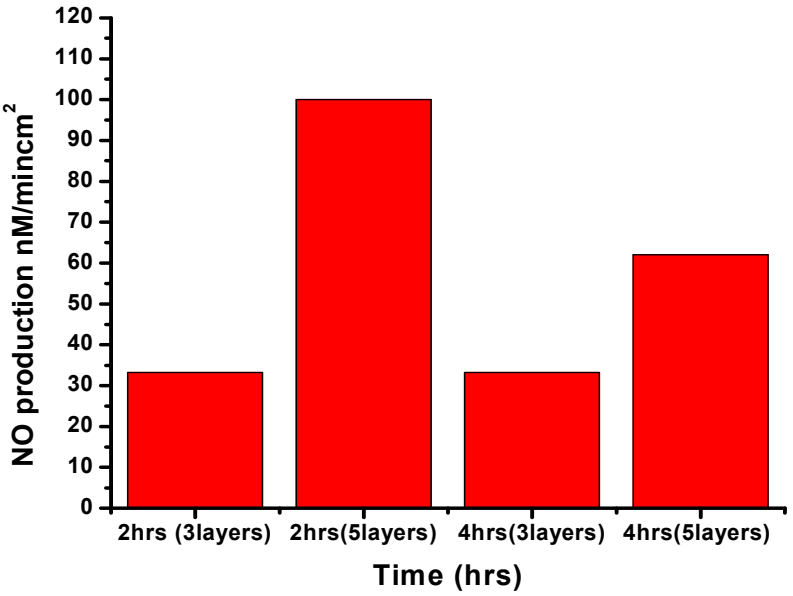

Figure 3.10: NO fluxes from PEI/NOS films with various thicknesses as determined by the Griess assay. The PEI/NOS film is composed of 3 and 5 layers of NOS enzyme sandwiched between alternate PEI polymer layers; time= 2hrs & 4hrs

Our results with 3 and 5 PEI/NOSoxy layers show that fluxes of NO release correlate with the number of enzyme layers present in the film. Increasing the number of iNOSoxy layers deposited within the PEI film yields higher NO fluxes, indicating the ability of our approach to fine-tune NO fluxes to meet requirements of optimum release for varying applications. This work shows a proof of principle strategy to use NOS enzymes in biocompatible films to release NO. These functional films would thus counteract thrombosis on blood-contacting devices. A similar work using the full length NOS with its reductase and oxygenase domains will be presented in the next chapter and show that NO can be similarly produced using the substrate arginine and the native NADPH as a source of electrons.

3.3 CONCLUSIONS

We have presented a proof of principle of a new approach for making antithrombotic coatings for medical devices and implants based on NO release. Our alternative approach is based on using nitric oxide synthase enzyme as the functional unit in a polymeric film for catalytic production of NO. The approach can use endogenous compounds for

continuous NO release from biocompatible films under physiologic conditions. We have demonstrated that NOS-based polymetric films successfully generate NO under physiologic condition at levels higher than those observed for endothelial cells. The level of NO release can be tuned through varying the number of NOS layers in the film buildup. We have shown that NO fluxes from our NOS-based PEI films are sustained for prolonged periods of time, which has the potential of producing efficient, long-term, antithrombotic coatings for medical devices and blood-contacting tools such as stents and catheters.

3.4 REFERENCES

1. Roy-Chaudhury P, Kelly BS, Zhang J, Narayana A, Desai P, Melham M, et al. Hemodialysis vascular access dysfunction: from pathophysiology to novel therapies. Blood Purif 2003;21(1):99-110.
2. Farrar DJ. Development of a prostethic coronary bypass graft. Heart Surg Forum 2000;3:36-40.
3. Eagleton MJO, K. Shortell, C. Green, R.M. Femoral-infrapopliteal bypass with prostethic grafts. Surgery 1999;126:759-765.
4. Schwartz RS, Holmes DR, Jr., Topol EJ. The restenosis paradigm revisited: an alternative proposal for cellular mechanisms. J Am Coll Cardiol 1992;20(5):1284-93.
5. Majerus PWB, G.J. Miletich, J.P.Tollefsen, D.M. Anticoagulant, thrombolytic and anitplatelet drugs. New York: Pergamon Press; 1991.
6. Cheung PY, Salas E, Schulz R, Radomski MW. Nitric oxide and platelet function: implications for neonatology. Semin Perinatol 1997;21(5):409-17.

7. Freedman JE, Loscalzo J, Barnard MR, Alpert C, Keaney JF, Michelson AD. Nitric oxide released from activated platelets inhibits platelet recruitment. J Clin Invest 1997;100(2):350-6.
8. Lvov YA, K. Ichinose, I. Kunitake, T. Assembly of Multicomponent Protein Films by Means of Electrostatic Layer-by-Layer Adsorption. Journal of the American Chemical Society 1995;117(22):6117-23.
9. Walford G, Loscalzo J. Nitric oxide in vascular biology. J Thromb Haemost 2003;1(10):2112-8.
10. Ignarro L. Biological actions and properties of endothelium-derived nitric oxide formed and released from artery and vein. Circ Res 1989;65:1-21.
11. Azuma HI, M. Sekizaki, S. Endothelium-dependant inhibition of platelet aggregation. Br J Pharmacol 1986;88:411-5.
12. Freedman JE, Sauter R, Battinelli EM, Ault K, Knowles C, Huang PL, et al. Deficient platelet-derived nitric oxide and enhanced hemostasis in mice lacking the NOSIII gene. Circ Res 1999;84(12):1416-21.
13. Zhou Q, Hellermann GR, Solomonson LP. Nitric oxide release from resting human platelets. Thromb Res 1995;77(1):87-96.

14. Malinski T, Radomski MW, Taha Z, Moncada S. Direct electrochemical measurement of nitric oxide released from human platelets. Biochem Biophys Res Commun 1993;194(2):960-5.
15. MacAllister RJ, Vallance P. The L-arginine nitric oxide pathway in the human cardiovascular system. J Int Fed Clin Chem 1996;8:152-158.
16. Radomski MWM, S. The biological and pharmacological role of nitric oxide in platelet function. Adv Exp Med Biol 1993;344:255-261.
17. Vaughn MW, Kuo L, Liao JC. Estimation of nitric oxide production and reaction rates in tissue by use of a mathematical model. Am J Physiol 1998;274(6 Pt 2):H2163-76.
18. Zhang H, Annich GM, Miskulin J, Osterholzer K, Merz SI, Bartlett RH, et al. Nitric oxide releasing silicone rubbers with improved blood compatibility: preparation, characterization, and in vivo evaluation. Biomaterials 2002;23(6):1485-94.
19. Frost MC, Reynolds MM, Meyerhoff ME. Polymers incorporating nitric oxide releasing/generating substances for improved biocompatibility of blood-contacting medical devices. Biomaterials 2005;26:1685-1693.

20. Matkrides SCR, U.S. Overview of the endothelium. In: Loscalzo JS, A.I., editor. Thrombosis and hemorrhage. Baltimore: Williams & Wilkins; 1998. p. 295-306.
21. Kelm M, Yoshida K. In: Feelisch M, Stamler JS, editors. Methods in Nitric Oxide Research. New York: John Wiley; 1996. p. 47-58.
22. Smith DJ, Chakravarthy D, Pulfer S, Simmons ML, Hrabie JA, Citro ML, et al. Nitric oxide-releasing polymers containing the [N(O)NO]-group. J Med Chem 1996;39(5):1148-56.
23. Wu Y, Rojas AP, Griffith GW, Skrzypchak AM, Lafayette N, Bartlett RH, et al. Improving blood compatibility of intravascular oxygen sensors via catalytic decomposition of S-nitrosothiols to generate nitric oxide in situ. Sensors and Actuators B: Chemical
Special Issue: 25th Anniversary of Sensors and Actuators B: Chemical 2007;121(1):36-46.
24. Hrabie JA, Keefer LK. New nitric oxide-releasing zwitterions derived from polyamines. J Org Chem 1993;58:1472-6.
25. Jourd'heuil D, Hallen K, Feelisch M, Grisham MB. Dynamic state of S-nitrosothiols in human plasma and whole blood. Free Radic Biol Med 2000;28(3):409-17.

26. Tyurin VA, Tyurina YY, Liu SX, Bayir H, Hubel CA, Kagan VE. Quantitation of S-nitrosothiols in cells and biological fluids. Methods Enzymol 2002;352:347-60.
27. Kader KN, Akella R, Ziats NP, Lakey LA, Harasaki H, Ranieri JP, et al. eNOS-overexpressing endothelial cells inhibit platelet aggregation and smooth muscle cell proliferation in vitro. Tissue Eng 2000;6(3):241-51.
28. Dong CH, Yuan XY, He MY, Yao KD. Preparation of PVA/PEI ultra-fine fibers and their composite membrane with PLA by electrospinning. Journal of Biomaterials Science-Polymer Edition 2006;17(6):631-643.
29. Zhou Z, Annich GM, Wu Y, Meyerhoff ME. Water-soluble poly(ethylenimine)-based nitric oxide donors: preparation, characterization, and potential application in hemodialysis. Biomacromolecules 2006;7(9):2565-74.
30. Bayachou M, Boutros J. Manuscript in preparation.
31. Ghosh DK, Wu C, Pitters E, Moloney M, Werner ER, Mayer B, et al. Characterization of the inducible nitric oxide synthase oxygenase domain identifies a 49 amino acid segment required for subunit

dimerization and tetrahydrobiopterin interaction. Biochemistry 1997;36(35):10609-19.

32. Raman CSL, H. Martasek, P. Kral, V. Masters, B.S. Poulos, T.L. Crystal structure of constitutive endothelial nitric oxide synthase: a paradigm for pterin function involving a novel metal center. Cell 1998;95:939.

33. Zhou LR, J.F. Detection of chemically induced DNA damage in layered films by catalytic square wave voltammetry using Ru(Bpy)32+. Anal Chem 2001;73:4780-4786.

34. Zhang XB, M. Amperometric detection of Nitric Oxide. Mod. Asp. Immunobiol. 2000;1(4):160-165.

35. Bayachou M, Lin R, Cho W, Farmer PJ. Electrochemical Reduction of NO by Myoglobin in Surfactant Film: Characterization and Reactivity of the Nitroxyl (NO⁻) Adduct. J. Am. Chem. Soc. 1998;120(38):9888-9893.

36. Immoos CE, Chou J, Bayachou M, Blair E, Greaves J, Farmer PJ. Electrocatalytic Reductions of Nitrite, Nitric Oxide, and Nitrous Oxide by Thermophilic Cytochrome P450 CYP119 in Film-Modified Electrodes and an Analytical Comparison of Its Catalytic Activities with Myoglobin. J. Am. Chem. Soc. 2004;126(15):4934-4942.

37. Crane BR, Arvai AS, Gachhui R, Wu C, Ghosh DK, Getzoff ED, et al. The structure of nitric oxide synthase oxygenase domain and inhibitor complexes. Science 1997;278(5337):425-31.
38. Sauerbrey G. The use of quartz oscillators for weighing thin layers and for microweighing. Zeitschrift fuer Physik 1959;155:206-22.
39. Schnell ZBVL, A.M. Kranpitz, T.R. Amino Acid Screen, Blood. In: F.A.Davis, editor. Davis's comprehensive handbook of Laboratory and diagnostic tests with nursing implications; 2003.
40. Clague MJW, J.S. Marletta, M.A. Formation of N-cyanoornithine from N-hydroxy-L-arginine and hydrogen peroxide by neuronal nitric oxide synthase: implications for mechanism. Biochemistry 1997;36:14465-14473.
41. Jun H-W, Taite LJ, West JL. Nitric Oxide-Producing Polyurethanes. Biomacromolecules 2005;6(2):838-844.
42. Miller PE, Carlton D, Deierhoi MH, Redden DT, Allon M. Natural history of arteriovenous grafts in hemodialysis patients. Am J Kidney Dis 2000;36(1):68-74.

CHAPTER IV

NO-RELEASE NITRIC OXIDE SYNTHASE-BASED BIOPOLYMERS

4.1 INTRODUCTION

Graft thrombosis is the cause of 80% of vascular access dysfunction, a problem with an associated health-care cost of over $1 billion/year [1]. The number of revascularization procedures have increased dramatically, and is estimated at 15% after initial coronary revascularization, and approximately 50% after lower extremity bypass [2,3]. Stent restenosis occurs at 30% of implant sites as a result of initial vascular thrombosis followed by cell proliferation, requiring a repeat angioplasty procedure within 1 year [4].

The thrombogenic nature of various polymeric materials utilized to prepare blood-contacting and implantable medical devices such as vascular grafts, intravascular catheters, sensors, coronary artery and vascular stents, and a host of other medical tools, even if labeled as biocompatible, can cause serious complications in patients. Thrombus formation at the surface of implantable medical devices is the major cause of vascular access dysfunction requiring secondary vascular procedures. Upon introduction of a foreign material into the blood stream, key proteins of the coagulation cascade (fibrinogen, and von Willebrand's factor) adsorb on the surface, followed by platelet adhesion and activation, leading to fibrin and thrombus formation at the surface (Figure 4.1).

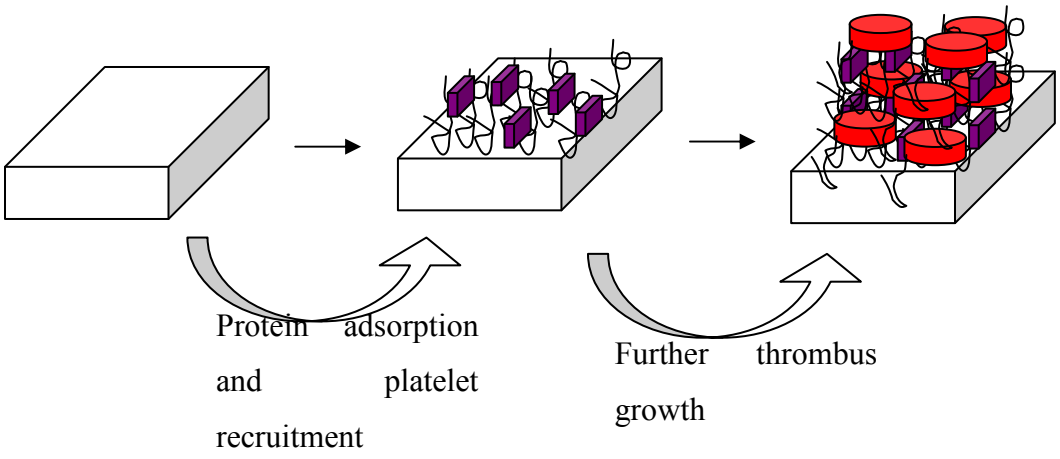

Figure 4.1: Illustration showing thrombus formation at the surface of implantable medical devices. Upon exposure to blood, protein adsorption occurs, followed by platelet adhesion at the surface. Platelet activation leads to thrombus formation at the surface.

An anti-coagulation regiment, with the adverse effects associated with long term use, is typically required to clinically reduce the risk of thrombus formation [5]. Thrombus formation involves two synergistic events; a cGMP-dependant mechanism that involves platelet activation, adhesion and aggregation [6], and fibrin formation resulting from the binding of bivalent fibrinogen to glycoprotein IIb/IIIa [7].

Nitric oxide (NO), a molecule generated by the enzyme Nitric Oxide Synthase (NOS) using L-arginine as a substrate, was recently identified as a potent antiplatelet agent. This small molecule orchestrates a myriad of vital physiological functions. For instance, the endothelium-derived NO production at low concentrations (nanomolar) plays a critical role in the regulation of vascular hemostasis [8], and inhibits platelet adhesion [9], and aggregation [10], as well as their further recruitment to the growing thrombus [11]. There have been numerous reports indicating NO release from resting [12], and aggregating platelets [13]. NO flux from activated human platelets have been indirectly measured and is estimated at ~1.2 $pmol.min^{-1}/10^8$ cells [12]. NO temporarily inactivates platelets in the close proximity of the endothelium [14]. This inhibition is short-lived and NO is rapidly scavenged by oxygen and hemoglobin in plasma [15]. To maintain this vital function and counteract thrombus

formation, stimulated human endothelial cells continuously generate NO at a level of *ca.* $4x10^{-10}$ $mol.cm^{-2}$ min^{-1} [16]. In this regard, NO-releasing bio-polymers are targeted as effective anti-thrombotic coatings in an attempt to enhance thromboresistivity of blood-contacting medical devices and implants.

Numerous approaches are investigated in an attempt to develop polymeric materials that are more blood-compatible. In general, these approaches can be categorized into two main trends: first, methods that mimic the anti-thrombogenic properties of endothelial cells [17], and, second, methods that use modified chemical surfaces and added moieties that limit protein and cell adhesion [18]. Prevention of protein adhesion *in vivo* is generally difficult to achieve, therefore the other approach, which aims at the development of surfaces mimicking properties of native endothelial cells, appears more promising. Nitric oxide, thrombomodulin, prostacyclin, and heparans contribute to the non-thrombogenic properties of the endothelial cells [19]. A potential solution can be found in polymeric coating materials that are capable of releasing low levels of nitric oxide at the blood/coating interface. Considerable efforts in this research area are focused on improving the NO-release chemistry of materials used as outer coatings for implantable medical

devices. Polymers that possess chemical platforms with the ability of releasing NO have been shown to exhibit varying levels of thromboresistivity. In fact, akin to nitric oxide-releasing endothelial cells, NO-releasing polymers as functional coatings have the potential to be effective in preventing platelet adhesion, activation, and aggregation onto surfaces. These coatings have the potential of reducing the risk of thrombus formation at the exterior of blood-contacting devices and implants. They also have the potential to prolong vascular graft and stent potency without adverse systemic effects [20]

Two classes of NO-releasing materials have been explored. N-diazeniumdiolate based NO-releasing polymers [21], and Nitrosothiol-based NO-releasing polymers [22]. N-diazeniumdiolates are inorganic NO donors formed by the reaction of a secondary amine structure with 2 equivalents of NO gas under high pressure, creating a relatively stable adduct structure [23]. The general structural types of diazeniumdiolates used for NO-releasing polymers include dispersed non covalently bound small molecules where the diazeniumdiolate group is attached to amines in low molecular weight compounds, and covalently bound diazeniumdiolates group to polymeric side chains or to the polymeric backbone [21].

The second class of proposed NO donors are S-nitrosothiols [24]; they mimic biological systems that are thought to serve as a NO reservoirs and transporters, such as S-nitroso-albumin and S-nitrosoglutathione, which are the most abundant naturally occurring S-nitrosothiols circulating in blood [25].

While films made of NO-donors incorporated into polymeric matrices did show the functional worthiness of NO-releasing coatings, this approach naturally results in only finite NO reservoirs, and thus the corresponding coatings are limited in their ability to sustain antithrombotic function over prolonged periods of time. The finite NO reservoir approach will also limit the potential use in more permanent types of implants. In addition, the NO fluxes achieved so far are lower than NO released from endothelial cells [18]. The logical alternative is then to explore approaches that would lead to materials with the ability to sustain NO generation for longer durations and at levels comparable to stimulated human endothelial cells (*ca.* $4x10^{-10}$ $molcm^{-2}min^{-1}$) [16], and/or potentially tunable levels.

Developing NO-releasing surfaces that closely resembles the endothelium is critical to achieving better thromboresistivity. The endothelial isoform of the enzyme nitric oxide synthase, eNOS, is a key

component of the endothelial cell lining. It was reported that eNOS-overexpressing endothelial cells seeding of synthetic small diameter vascular grafts decreased human platelet aggregation by 46%, and bovine aortic smooth muscle cell proliferation by 67.2% *in vitro* [26]. NO-releasing materials using polyethyeleneimine (PEI), a biocompatible polymer [27], has been reported in literature [28]. In our lab, NO was successfully generated from the enzyme nitric oxide synthase embedded in bilayered cast surfactant films [29].

NO releasing materials using Polyethyeleneimine (PEI), a biocompatible polymer [27], has been reported in literature [28,30,31]. In our lab, NO was successfully generated nitric oxide from the oxygenase domain of the enzyme Nitric Oxide Synthase (NOSoxy) embedded in polymeric matrix by means of layer-by-layer electrostatic adsorption [32,33]. In this work, we incorporated the enzyme nitric oxide synthase in the PEI polymeric matrix by means of layer-by-layer electrostatic adsorption [33], to construct a multicomponent protein film that mimics the NO-generating behavior of the endothelial cell lining. We demonstrate in this paper that our films provide a viable source of NO that utilizes endogenous compounds to maintain a continuous supply of nitric oxide.

4.2 MATERIALS AND METHODS

4.2.1 EXPRESSION AND PURIFICATION OF iNOS VIA RECOMBINANT PLASMID DNA

Many proteins and enzymes can be purchased through chemical catalogs with moderate expense making them best procured through those sources. NOS is not one of them. Because of the small biological quantities found in animal tissue, preparation and purification from biological sources would be prohibitively expensive. Making the procurement even more prohibitive is the fact that we need to specifically target the oxygenase domain of the enzyme, which could be obtained separate from the reductase domain by limited proteolysis of the full-length strand. However, to use NOS enzyme in the quantities required for the completion of the current study requires an unbroken, relatively inexpensive source of enzyme without the tedious extra steps involved with enzyme proteolysis. This is accomplished through in-house protein expression and purification of the full-length enzyme via recombinant plasmid DNA.

The pCWori vector, a generous gift from the laboratory of Dennis Stuehr at the Lerner Research Institute, is inserted into plasmid DNA and transformed into BL21 (DE3) ampicillin-resistant *E. coli* as detailed by the Stuehr group [34]. This glycerol stock is then inoculated into 2 x 2 ml LB medium with 100 μg/ml added ampicillin and chloramphenicol, and allowed to grow overnight at 37°C.

Each aliquot of overnight culture is added to 500 ml autoclaved TB solution and allowed to grow under agitation at 37°C for about 3 hours or until 0.1 OD_{600} is reached. Temperature is dropped to 25°C until 0.3 – 0.8 OD_{600} is reached, at which time IPTG and δ-aminolevulinic acid are added to induce iNOS protein production and to provide a heme precursor for the metalloprotein. The induced culture is left again overnight to produce maximum quantities of protein. Cells are harvested by centrifugation at 4,000 rpm at 4°C for 30 minutes, drained of supernate, and resuspended in a minimum of pH 7.6 lysis buffer containing base buffer, lysozyme, phenylmethanesulfonylfluoride (PMSF), Protease Inhibitor III (4-(2-Aminoethyl) benzenesulfonyl fluoride hydrochloride, aprotinin, leupetin, pepstatin A, bestatin, and L-3-trans-Carboxyoxiran-2-carbonyl)-L-leucyl-agmatin), DNase, and $MgCl_2$. Cells are lysed by sonication at 15-second on, 45-second off intervals for

a period of twenty minutes. The sonicated suspension is centrifugated at 12,000 g at 4°C for 30 minutes to precipitate cellular debris. The debris pellet is discarded and the crude supernatant lysate is collected. Protein precipitation is induced by gradual addition of 0.300 g $(NH_4)_2SO_4$/ml over a period of 1 hour followed by centrifugation at 10,000 rpm to collect the protein pellet. The pellet is again resuspended in base buffer, PMSF, and Protease Inhibitor III and filtered through a 0.45 micron PES syringe filter. A 4 ml dead volume Ni-NTA Agarose column is prepared for use by charging with 50 mM $NiSO_4$, followed by addition of a binding tris buffer before loading the filtered protein sample onto the column. The column is equilibrated with tris binding buffer and washed with a dilute (40 mM) imidazole wash buffer prior to elution with c. 200 mM imidazole elution buffer. The protein was collected off the column and dialyzed in 500 ml base buffer with 200 µl β-mercaptoethanol, changing dialysis solution twice during the overnight process. The dialyzed protein is further concentrated by centrifugation at 5000 rpm at 4°C using 30,000 MW cut-off Amicon filters until the desired concentration (usually 0.45 mM) is reached. Aliquots of the protein are stored at -80°C for future use. Protein concentration is determined by Bradford assay and by UV-Vis analysis of the Soret band at 421 nm.

SDS-PAGE further confirms the presence of iNOS by marker comparison to molecular weight standards.

4.2.2 PREPARATION OF PEI/NOS FILM

The full length inducible nitric oxide synthase (iNOS) was expressed in house as reported in literature [35]. A pyrolytic graphite surface (unless indicated otherwise) was initially modified utilizing our diazonium method as described in the literature to obtain a uniform negative charge at the surface [36]. Typically, the PG surface is dipped in a mixture of 50mM p-aminobenzoate and 50mM sodium nitrite at 4˚C, in a 3 necked electrochemical cell. The potential is scanned between 0 and -0.6 V vs Ag/AgCl leading to the covalent attachment of diazonium group on the surface, with a free carboxylic group (COO^-). The pyrolytic graphite surface was alternatively dipped coated in a polyethyleneimine (PEI; 1.5mg/ml) solution and iNOS solution for 10 minutes respectively to achieve the desired film composition. The surface was thoroughly washed with deionized and air-dried after each step. The films were stored overnight at 4°C. (Figure 4.2)

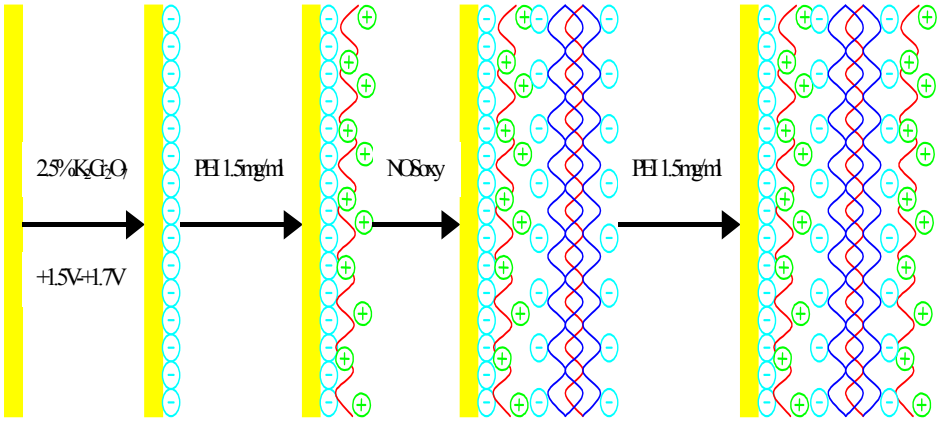

Figure 4.2: Assembly of PEI/NOS film using layer-by-layer electrostatic deposition.

4.2.3 QUARTZ CRYSTAL MICROBALANCE (QCM) CHARACTERIZATION

QCM analysis was carried out at the surface of a thin oscillating quartz crystal sandwiched between two gold electrodes. Prior to coating, the quartz crystal surface surface was cleaned by soaking in a piranha solution (30%H_2O_2; 70%H_2SO_4) for 5 minutes, followed by rinsing with deionized water, and dried under nitrogen. The surface of the quartz crystal was modified, prior to deposition, with our diazonium method as previously described. We measured the reduction in resonance frequency with each deposited layer and calculated the mass deposited using the Sauerbrey equation, which directly relates the decrease in frequency to mass change [37]. QCM analysis was performed on a CH Instrument electrochemical workstation using a QCM cell; the same cell was used for electrochemical experiments needed to modify the gold surface prior to LBL depositions.

4.2.4 ATOMIC FORCE MICROSCOPY

Atomic Force Microscopy characterization was carried out at the surface of 1cmx1cm highly oriented pyrolytic graphite (HOPG) slides. Initially, the top layer on the slide was peeled to eliminate any interference from dust particles. The HOPG surface was modified with the diazonium method as previously described. The surface was modified as previously described and images were taken following each layer deposition using a Molecular Imaging pico-SPM using the MAC mode interfaced with a PicoScan controller (MICorp, Arizona).

4.2.5 NO FLUX MEASUREMENTS

The films were prepared as described above. We prepared reaction cocktail composed of the substrate L-arginine at physiological levels (100μM) [38], 1mM Calcium Chloride ($CaCl_2$) in Phosphate buffer (100mM; pH=7.4). NADPH (150μM) was used as a source of reducing equivalents, which is widely used in the NOS community. The enzymatic reaction was run at 37°C for the desired time period. The enzymatic activity of the film at the pyrolytic graphite surface was quantified by

measuring NO flux using the Griess assay [39,40]. Absorbance measurements were taken using an Agilent 8543 Spectrophotometer utilizing 1-cm path UV-visible cells.

4.2.6 PLATELET ADHESION STUDIES

Whole blood from dog was drawn into blood collection tubes containing 60 units of sodium heparin as an anticoagulant. The heparinized whole blood was centrifuged at 110g for 15 min at 228C. platelet-rich plasma (PRP) was collected from the supernatant. To re-establish platelet activity, $CaCl_2$ was added to the PRP to raise [Ca^{2+}] by 2 mM. Before PRP incubation, the Indium Tin Oxide (ITO) slides were modified by the method described previously. Then, the polymer coated ITO slides were incubated for 1 h at 37˚C in 500 mL of recalcified PRP under static conditions. The PRP was then decanted and the wells were washed once with 200 mL PBS.

4.2.7 LACTATE DEHYDROGENASE ASSAY

Before PRP incubation, the poly-L-Lysine coated microtiter plate wells were modified by the method described previously. Then, 100 mL of recalcified PRP was added to each polymer-coated well and incubated for 1 h at 37˚C under static conditions. The PRP was then decanted and the wells were washed once with 200 mL PBS. Adhered platelets were lysed using a lysing buffer which was 1% (w/v) Triton X-100. 150μL of lysing buffer was incubated in each well for 1 h at 37˚C with occasional agitation to completely disrupt the platelet membranes. Then, 100 μL of each lysate solution was pipetted into wells of a 96-well polystyrene microtiter plate (Fisher) that contained 100 μL of reagent from an LDH assay kit (Roche Applied Sciences, Indianapolis, IN), and incubated for 30 min at 25˚C. Then, 50 μL of stop solution is added and absorbance of each well at 490 nm was monitored by a Labsystems Multiskan RC microplate reader.

4.3 RESULTS AND DISCUSSION

4.3.1 QUARTZ CRYSTAL MICROBALANCE (QCM) CHARACTERIZATION

Quartz Crystal Microbalance (QCM) was used as a tool to investigate mass changes upon the alternate deposition of PEI and the iNOS enzyme. QCM analysis was carried out at the surface of a thin oscillating quartz crystal sandwiched between two gold electrodes. The measurement of the resonant frequency changes at the surface of a modified quartz crystal with the alternate deposition of PEI and iNOS at the surface of a quartz crystal indicates a decrease in frequency that correlates with mass increase at the surface. Figure 4.4 indicates a typical QCM plot of the frequency change ΔF_0 upon the alternate deposition of PEI and the NOS enzyme on a quartz crystal. The average change in frequency per layer deposited is ΔF_0= 58 Hz as indicated by Figure 4.3.

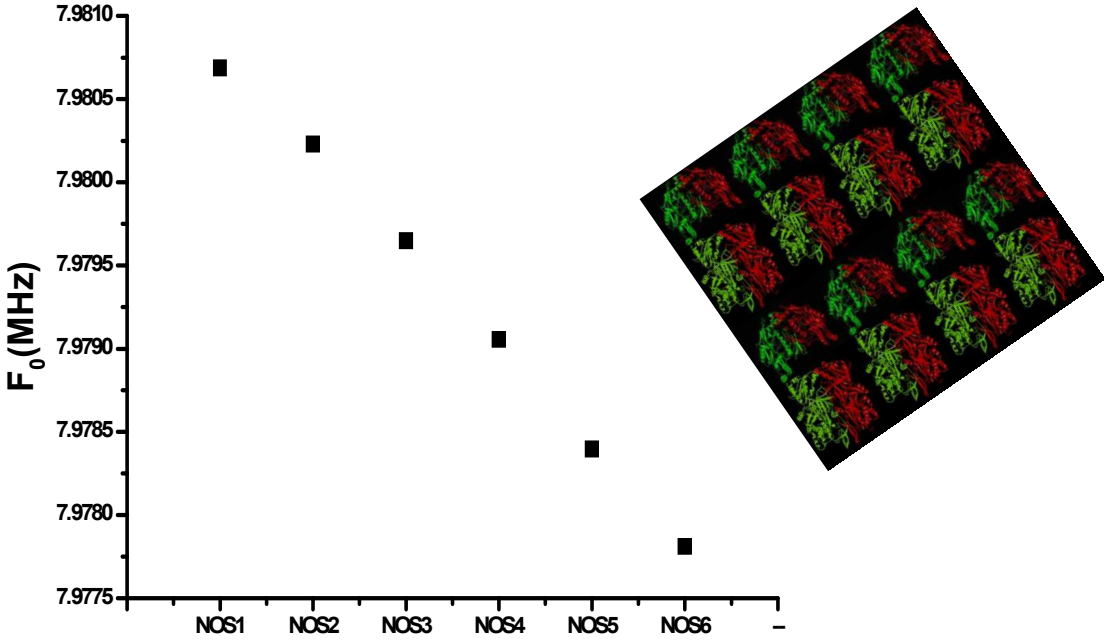

Figure 4.3: A- Monitoring of the PEI/NOS multilayer film building through the layer-by-layer methodology using quartz crystal microbalance. B- Proposed model based on measured changes in crystal frequency showing that iNOSoxy in a monolayer of dimers in each layer of iNOSoxy in the LBL process.

The change in frequency can be converted to mass changes by the Sauerbrey equation [37]. The mass change obtained in addition to the known dimensions of the iNOS enzyme (120x80x60 Å), and the molecular weight of the iNOS (120kDa) allows the determination of a model of the enzyme orientation within the PEI film. A monolayer of iNOS dimers (as seen in Figure 4.3B) corresponds to a theoretical ΔF_0= 60 Hz which is of the same magnitude as the ΔF_0 seen experimentally. iNOS is catalytically active in the dimeric form hence indicating that the charge-dependant orientation of the enzyme within the PEI matrix is such to retain its function.

4.3.2 ATOMIC FORCE MICROSCOPY CHARACTERIZATION

To investigate the success of our methodology in producing polymeric film coatings with the desired coverage and surface morphology, we further characterized our LBL deposition of film components using atomic force microscopy (AFM) imaging. Figure 4.4 illustrates the AFM image of the layer-by-layer iNOS/PEI film buildup. Figure 4.4A illustrates the 3D AFM image of the deposition of a layer of the polymer PEI at the surface of the HOPG slide. The figure shows a

uniform spread of the PEI polymer on the surface. The surface height is of the order of 2.0nm. Figure 4.4B shows the 3D AFM image of the deposition of a layer of iNOS over a layer of the polymer PEI at the surface of the HOPG slide. The figure shows a uniform distribution of the enzyme over the surface. Closer analysis of the features that result upon exposure to iNOS solution confirms that the observed dimensions are close to the crystallographic dimension of iNOS [42]. The overall surface height is of the order of 8.0nm. Figure 4.4C shows the AFM image of the same HOPG slide after the sequential deposition of PEI over a layer of iNOS resulting in the PEI/iNOS/PEI coating. This image shows that the layer of iNOS is still present but is now embedded in between two alternate PEI layers. The biocompatible polymeric coat now brings the average surface height to the order of 10.0nm, which is consistent with the cumulative surface heights measured for the PEI layers an the layer of iNOS.

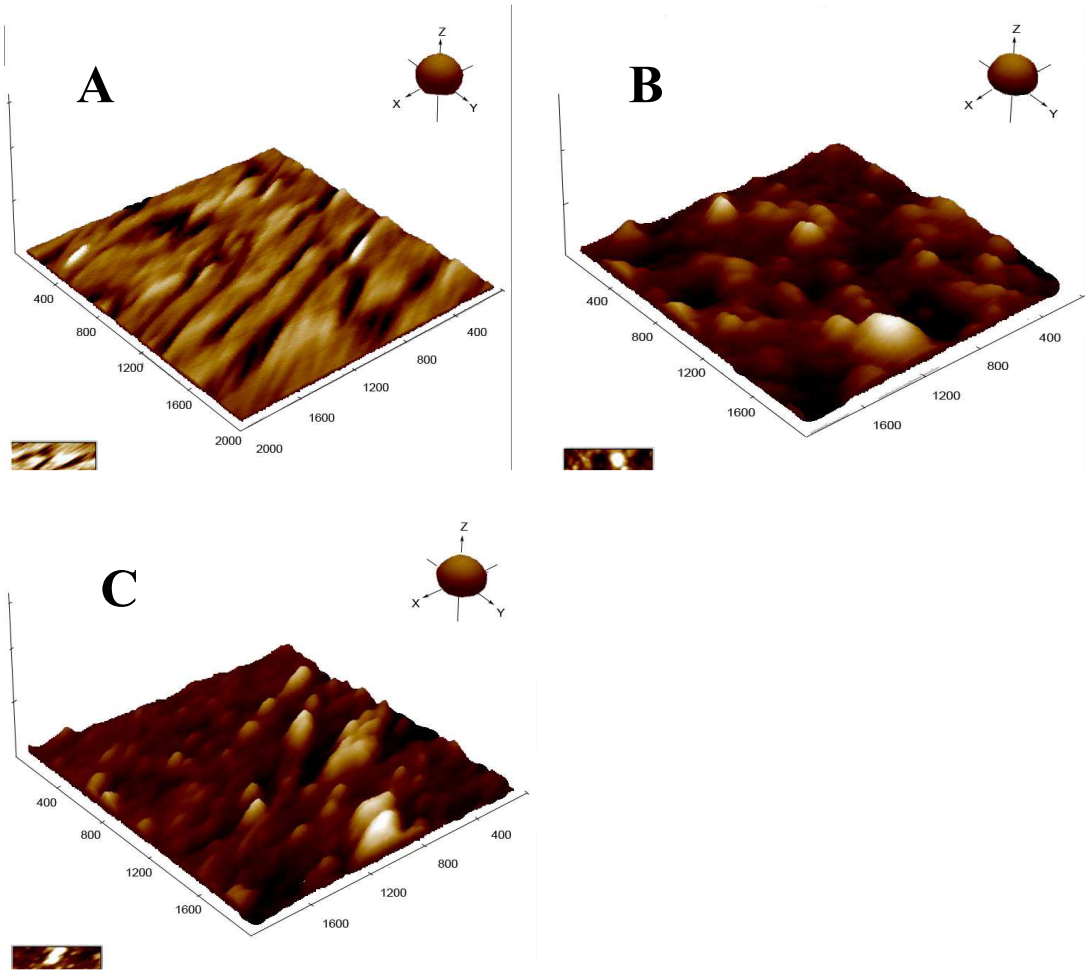

FIGURE 4.4: Atomic force microscopy images at the surface of highly oriented pyrolytic graphite (HOPG) depicting typical PEI/NOS film composition. (A) is a 2μmx2μm 3D scan of the layer of PEI polymer deposited at the HOPG surface. (B) is a 2μmx2μm 3D scan of a layer of NOS enzyme deposited over a layer of PEI polymer. (C) is a 2μmx2μm 3D scan of the final layer of PEI polymer deposited after the deposition of a NOS enzyme layer.

Our step-by-step AFM characterization shows that the functional component of our films, i.e. the iNOS enzyme, is successfully trapped in between layers of the PEI polymer. In addition, AFM imaging shows that our LBL methodology yields a thin film with uniform coverage of the surface. A uniform coverage of the surface is instrumental in efficiently prohibiting seed contacts at the blood/device interface, which will help improve the thromboresistivity of the device.

4.3.3 NO FLUX MEASUREMENTS

Successful NO release was achieved from our PEI/NOS films and at fluxes higher than what have been reported in the literature for other inorganic NO-releasing systems [18]. Typical substrates prepared as described above are utilized to investigate the NO production capability from the trapped iNOS enzymes. The enzymatic activity of the coatings at the pyrolytic graphite surface was quantified by measuring NO flux using the Griess assay [39, 40], which tracks the accumulation of nitrite as the decomposition product of NO generated by iNOS in the film. Figure 4.5 reveals total NO release from films composed of 5 consecutive layers of PEI/NOS. An increase in NO released is achieved with increasing time.

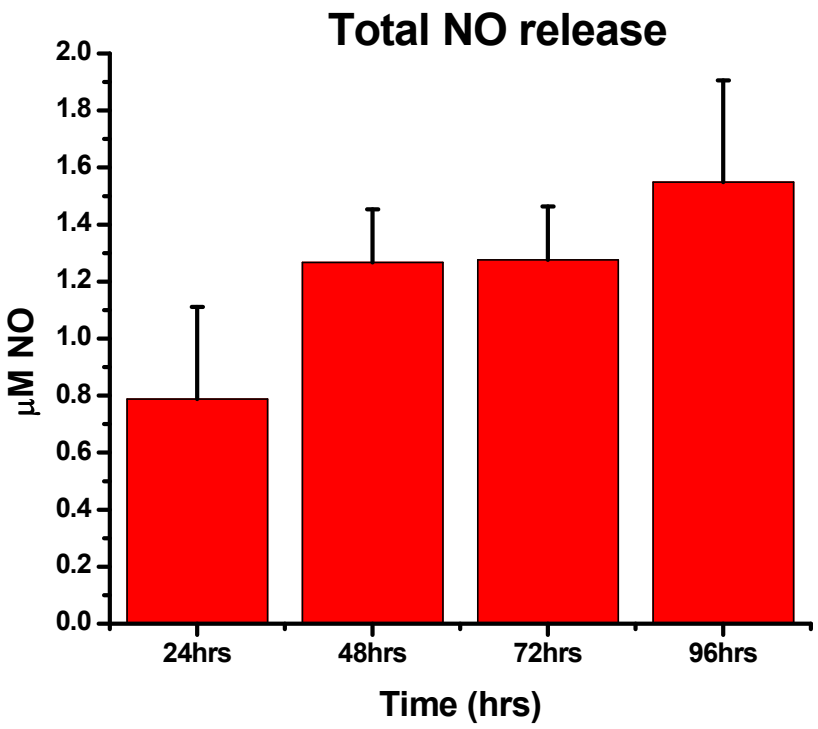

Figure 4.5: Total surface NO flux from PEI/NOS preparation as determined by the Griess assay. The PEI/NOS film is composed of 5 layers of NOS enzyme sandwiched between alternate PEI polymer layers. n=5

Figure 4.6 shows the cumulative NO production by the (PEI/iNOS) coating in terms of normalized NO surface flux. The figure shows that an initial burst of NO occurs at 24 hours (1.09nM $NO.min^{-1}.cm^{-2}$ ± 0.45; n=5), 48 hours (0.88nM $NO.min^{-1}.cm^{-2}$ ± 0.13; n=6), 72 hours (0.59nM $NO.min^{-1}.cm^{-2}$ ± 0.08; n=5), followed by a sustained release at 96 hours (0.54nM $NO.min^{-1}.cm^{-2}$ ± 0.12; n=5).

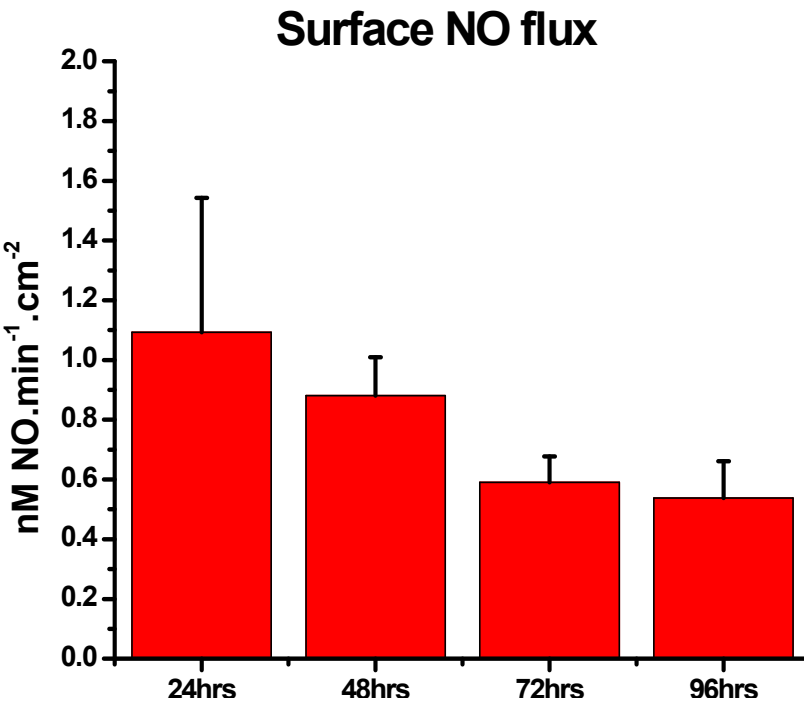

Figure 4.6: NO surface flux vs time from PEI/NOS preparation as determined by the Griess assay. The PEI/NOS film is composed of 3 layers of NOS enzyme sandwiched between alternate PEI polymer layers. n=5

Successful NO release was achieved from our PEI/NOS films and at fluxes higher than what have been reported in the literature for other inorganic NO-releasing systems [18]. Our PEI/iNOS film sustained catalytic production of NO for long periods of time and in conditions that mimic physiologic settings. Our enzyme-based NO production approach in the biocompatible PEI film closely mimics the behavior of endothelial cells and essentially overcomes the shortcoming of other approaches that result in only finite NO-reservoirs. Sustained NO fluxes were observed for a period of 96 hours. This initial burst eventually settles down at longer periods. NO release from PEI films shows 2-phase kinetics: an initial burst of NO, followed by a sustained release over a longer period of time. This 2-phase kinetics of NO release is in line with previously published studies [43]. The initial burst can be useful to counter early prosthetic graft occlusion that occurs in 18% of synthetic vascular access conduits for dialysis [44], and 25% of infrapoliteal synthetic grafts [3]. The PEI/NOS film has the ability to function as a thromboresistant scaffold that imitates the endothelial cell lining response through the biphasic NO release exhibited.

To monitor the effects of film thickness on NO fluxes we investigated NO release from films with varying numbers of iNOS layers. Figure 4.7 shows increased NO fluxes from a film composed of 5 layers of PEI/NOS relative to a film preparation of 3 layers, and 1 layer of PEI/NOS respectively, indicating that higher NO fluxes can be achieved by increasing the thickness, i.e. enzyme loading, of the polymeric coatings. The rate of NO release is crucial, and the optimum NO levels for coatings to be applied on medical devices and blood-contacting implants are yet to be determined. Therefore, the ability to control NO fluxes is of utmost importance. Our layer-by-layer approach provides the ability to control NO fluxes from films by varying the number of NOS enzyme layers in the polymeric matrix. In addition to producing nanometer-thick coatings, the layer-by-layer electrostatic self-assembly method has the built-in ability to tweak the film architecture to meet the requirements of thickness and composition.

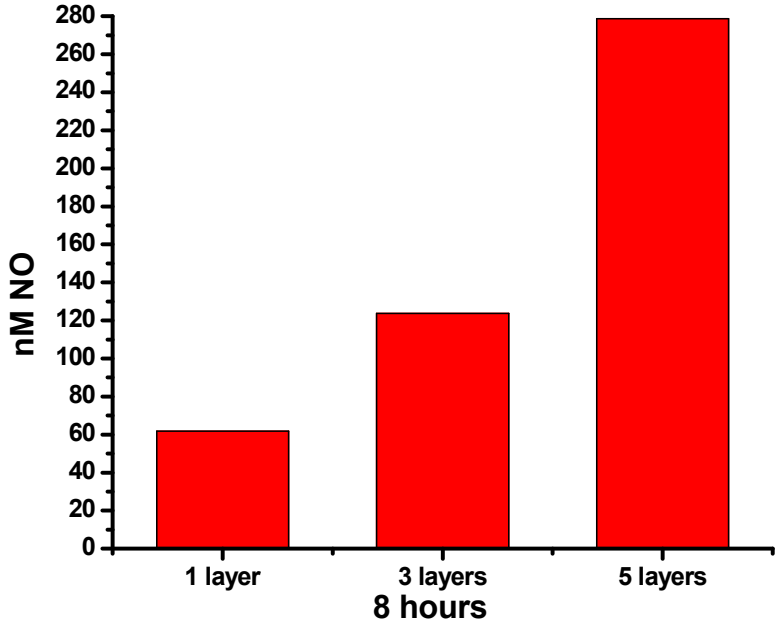

Figure 4.7: NO fluxes from PEI/NOS films with various thicknesses as determined by the Griess assay. The PEI/NOS film is composed of 1,3 and 5 layers of NOS enzyme sandwiched between alternate PEI polymer layers; time= 8hrs

Our results with 1, 3 and 5 PEI/NOS layers show that fluxes of NO release correlate with the number of enzyme layers present in the film. Increasing the number of iNOS layers deposited within the PEI film yields higher NO fluxes, indicating the ability of our approach to fine-tune NO fluxes to meet requirements of optimum release for varying applications.

4.3.4 PLATELET ADHESION STUDIES

To evaluate the thromboresistivity of the NOS based polymeric coatings *in vitro*, ITO slides, glass substrates that offer the advantage of being conductive, were coated with the NOS containing polymer (Figure 4.8B), as well as BSA containing polymer (Figure 4.8A) (negative control). Those slides were incubated with platelet rich plasma for 1 hour at 37°C, and then rinsed with PBS buffer. Phase contrast microscopy images of NO releasing NOS based polymers (Figure 4.8D) consistently showed almost no platelet adhesion at the surface when compared with a negative control (Figure 4.8C), indicating an overall enhancement of the thromboresistive properties of those coatings.

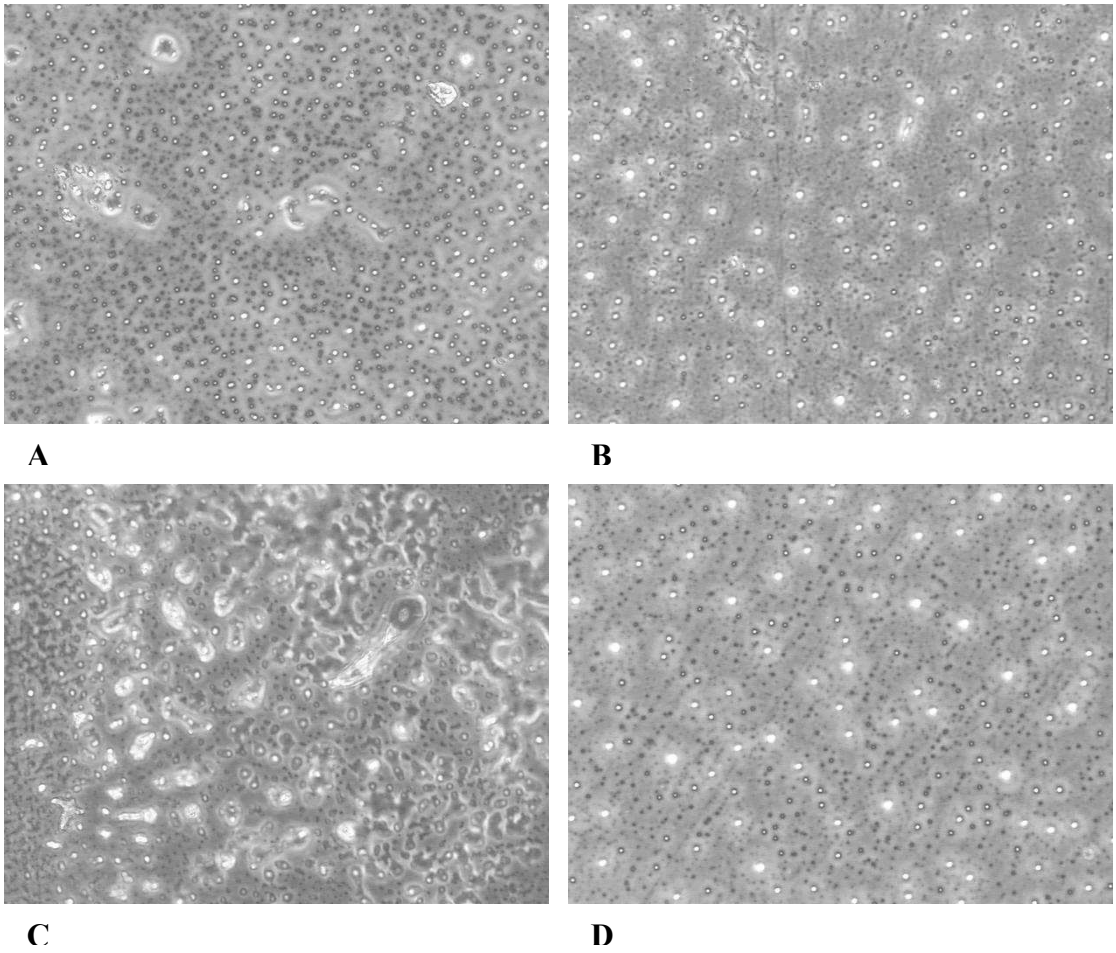

Figure 4.8: Phase contrast microscopy images pre-incubation of A) PEI/BSA film and B) PEI/NOS film, and post incubation with platelet rich plasma C) PEI/BSA film and D) PEI/NOS.

4.3.5 LACTATE DEHYDROGENASE ASSAY

LDH assay is useful in quantifying cell and platelet adhesion at the surface of the PEI/NOS coatings. LDH is an enzyme found in cells at levels proportional to its size [45], and is released following cell breakdown. *In vitro* determination of the degree of platelet adhesion to surfaces using LDH assay has been reported [45-47].

Figure 4.9 reveals the corresponding LDH level results of uncoated surface (bare) 0.16±0.04 (N=7), 5 layer coating (5 layers of NOS) 0.11±0.01 (N=7), and 10 layer coating (10 layers of NOS) 0.06±0.01 (N=7).

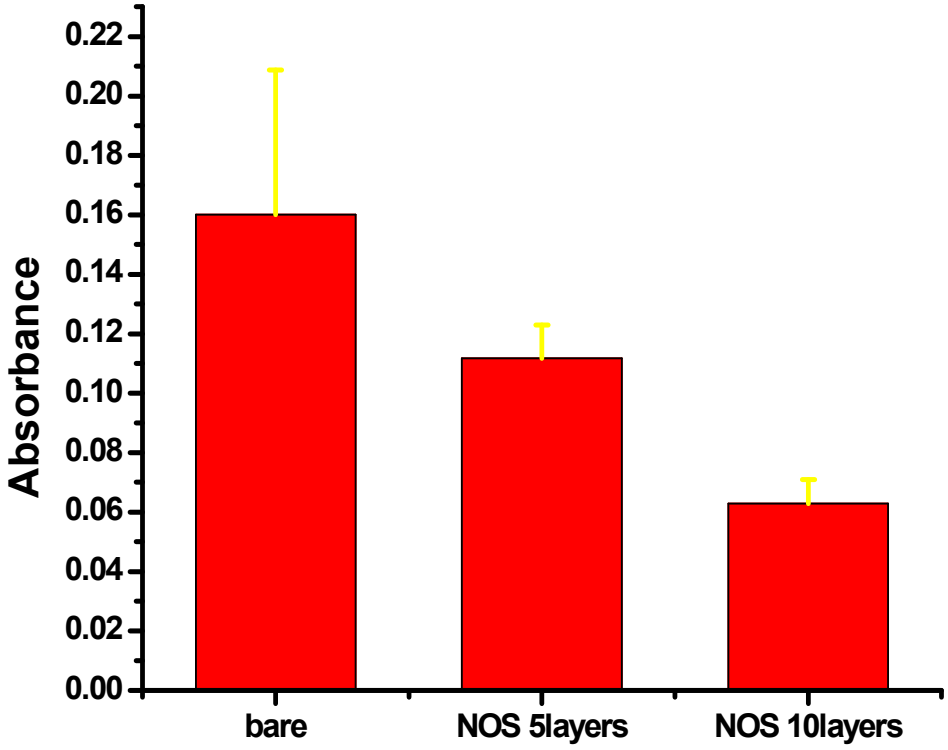

Figure 4.9: LDH assay of platelet adhesion on the surface of the PEI/NOS coatings.

In figure 4.10, the mean LDH activity at the bare surface was considered to correspond to 100% adhesion, and a decreased amount of adhered platelets was seen with the 5 layer coatings (69.8%) and with the 10 layer coatings (39.3%).

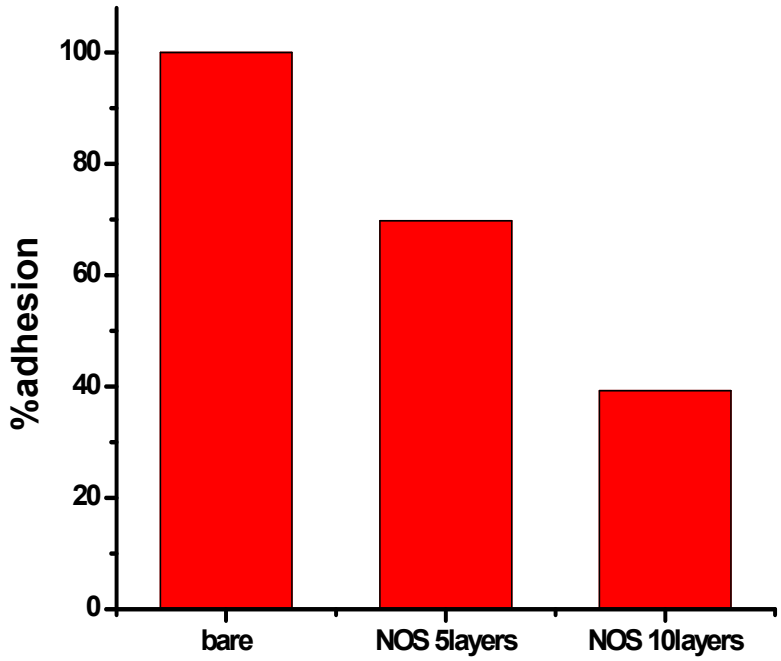

Figure 4.10: Percentage platelet adhesion on the surface of the PEI/NOS coatings.

As expected, the results presented reveals that the increasing number of NOS layers within the PEI/NOS coating corresponding to higher NO fluxes, reduced platelet adhesion *in vitro* up to 60.7%. The inhibition of platelet adhesion is a critical step in inhibiting thrombus formation at the surface of implantable medical devices. The enhanced thromboresistivity displayed by these coatings provide the basis of future endeavors in developing more biocompatible coatings for surface modifications of implantable medical devices.

4.4 CONCLUSIONS

Thrombus formation at the surface of implantable medical devices is the major cause of vascular access dysfunction requiring secondary vascular procedures. NO releasing bio-polymers are being sought as an effective anti-thrombotic coatings in an attempt to enhance thromboresistivity of those devices. The approaches utilizing NO-donors incorporated into polymeric matrices suffer from being a finite NO reservoir, and thus they are limited in their ability to sustain NO fluxes over a prolonged period of time. We presented a logical alternative that explores approaches aiming at developing materials with the ability to

sustain NO release for longer durations and at levels comparable to stimulated human endothelial cells ($0.5\text{-}4x10^{-10}$ $molcm^{-2}min^{-1}$) [16].

NOS based polyethyleneimine coatings were successfully developed with the layer-by-layer methodology. NO was successfully generated from these coatings at levels comparable to stimulated human endothelial cells. NO release from these NOS-based coatings successfully decreased platelet adhesion at the surface by 60%, which potentially might lead to improved thromboresistivity of implantable devices when coated with those materials.

4.5 REFERENCES

1. Roy-Chaudhury P, Kelly BS, Zhang J, Narayana A, Desai P, Melham M, et al. Hemodialysis vascular access dysfunction: from pathophysiology to novel therapies. Blood Purif 2003;21(1):99-110.
2. Farrar DJ. Development of a prostethic coronary bypass graft. Heart Surg Forum 2000;3:36-40.
3. Eagleton MJO, K. Shortell, C. Green, R.M. Femoral-infrapopliteal bypass with prostethic grafts. Surgery 1999;126:759-765.
4. Schwartz RS, Holmes DR, Jr., Topol EJ. The restenosis paradigm revisited: an alternative proposal for cellular mechanisms. J Am Coll Cardiol 1992;20(5):1284-93.
5. Majerus PWB, G.J. Miletich, J.P.Tollefsen, D.M. Anticoagulant, thrombolytic and anitplatelet drugs. New York: Pergamon Press; 1991.
6. Cheung PY, Salas E, Schulz R, Radomski MW. Nitric oxide and platelet function: implications for neonatology. Semin Perinatol 1997;21(5):409-17.

7. Freedman JE, Loscalzo J, Barnard MR, Alpert C, Keaney JF, Michelson AD. Nitric oxide released from activated platelets inhibits platelet recruitment. J Clin Invest 1997;100(2):350-6.
8. Walford G, Loscalzo J. Nitric oxide in vascular biology. J Thromb Haemost 2003;1(10):2112-8.
9. Ignarro L. Biological actions and properties of endothelium-derived nitric oxide formed and released from artery and vein. Circ Res 1989;65:1-21.
10. Azuma HI, M. Sekizaki, S. Endothelium-dependant inhibition of platelet aggregation. Br J Pharmacol 1986;88:411-5.
11. Freedman JE, Sauter R, Battinelli EM, Ault K, Knowles C, Huang PL, et al. Deficient platelet-derived nitric oxide and enhanced hemostasis in mice lacking the NOSIII gene. Circ Res 1999;84(12):1416-21.
12. Zhou Q, Hellermann GR, Solomonson LP. Nitric oxide release from resting human platelets. Thromb Res 1995;77(1):87-96.
13. Malinski T, Radomski MW, Taha Z, Moncada S. Direct electrochemical measurement of nitric oxide released from human platelets. Biochem Biophys Res Commun 1993;194(2):960-5.

14. MacAllister RJ, Vallance P. The L-arginine nitric oxide pathway in the human cardiovascular system. J Int Fed Clin Chem 1996;8:152-158.
15. Radomski MWM, S. The biological and pharmacological role of nitric oxide in platelet function. Adv Exp Med Biol 1993;344:255-261.
16. Vaughn MW, Kuo L, Liao JC. Estimation of nitric oxide production and reaction rates in tissue by use of a mathematical model. Am J Physiol 1998;274(6 Pt 2):H2163-76.
17. Zhang H, Annich GM, Miskulin J, Osterholzer K, Merz SI, Bartlett RH, et al. Nitric oxide releasing silicone rubbers with improved blood compatibility: preparation, characterization, and in vivo evaluation. Biomaterials 2002;23(6):1485-94.
18. Frost MC, Reynolds MM, Meyerhoff ME. Polymers incorporating nitric oxide releasing/generating substances for improved biocompatibility of blood-contacting medical devices. Biomaterials 2005;26:1685-1693.
19. Matkrides SCR, U.S. Overview of the endothelium. In: Loscalzo JS, A.I., editor. Thrombosis and hemorrhage. Baltimore: Williams & Wilkins; 1998. p. 295-306.

20. Kelm M, Yoshida K. In: Feelisch M, Stamler JS, editors. Methods in Nitric Oxide Research. New York: John Wiley; 1996. p. 47-58.

21. Smith DJ, Chakravarthy D, Pulfer S, Simmons ML, Hrabie JA, Citro ML, et al. Nitric oxide-releasing polymers containing the [N(O)NO]-group. J Med Chem 1996;39(5):1148-56.

22. Wu Y, Rojas AP, Griffith GW, Skrzypchak AM, Lafayette N, Bartlett RH, et al. Improving blood compatibility of intravascular oxygen sensors via catalytic decomposition of S-nitrosothiols to generate nitric oxide in situ. Sensors and Actuators B: Chemical

Special Issue: 25th Anniversary of Sensors and Actuators B: Chemical 2007;121(1):36-46.

23. Hrabie JA, Keefer LK. New nitric oxide-releasing zwitterions derived from polyamines. J Org Chem 1993;58:1472-6.

24. Jourd'heuil D, Hallen K, Feelisch M, Grisham MB. Dynamic state of S-nitrosothiols in human plasma and whole blood. Free Radic Biol Med 2000;28(3):409-17.

25. Tyurin VA, Tyurina YY, Liu SX, Bayir H, Hubel CA, Kagan VE. Quantitation of S-nitrosothiols in cells and biological fluids. Methods Enzymol 2002;352:347-60.

26. Kader KN, Akella R, Ziats NP, Lakey LA, Harasaki H, Ranieri JP, et al. eNOS-overexpressing endothelial cells inhibit platelet aggregation and smooth muscle cell proliferation in vitro. Tissue Eng 2000;6(3):241-51.

27. Dong CH, Yuan XY, He MY, Yao KD. Preparation of PVA/PEI ultra-fine fibers and their composite membrane with PLA by electrospinning. Journal of Biomaterials Science-Polymer Edition 2006;17(6):631-643.

28. Zhou Z, Annich GM, Wu Y, Meyerhoff ME. Water-soluble poly(ethylenimine)-based nitric oxide donors: preparation, characterization, and potential application in hemodialysis. Biomacromolecules 2006;7(9):2565-74.

29. Bayachou M, Boutros J. Manuscript in preparation.

30. Pulfer SKO, D. Smith, D.J. Incorporation of Nitric oxde-releasing crosslinked polyethyleneimine microspheres into vascular grafts. J Biomed Res 1997;37:182-189.

31. Bauer JA, Rao W, Smith DJ. Evaluation of linear polyethyleneimine/nitric oxide adduct on wound repair: therapy versus toxicity. Wound Repair Regen 1998;6(6):569-77.

32. Decher GH, J.D. Buildup of ultrathin multilayer films by a self-assembly process: II. Consecutive adsorption of anionic and cationic bipolar amphiphiles and polyelectrolytes on charged surfaces. Berichte der Bunsen-Gesellschaft 1991;95(11):1430-1434.
33. Lvov YA, K. Ichinose, I. Kunitake, T. Assembly of Multicomponent Protein Films by Means of Electrostatic Layer-by-Layer Adsorption. Journal of the American Chemical Society 1995;117(22):6117-23.
34. Ghosh DK, Wu C, Pitters E, Moloney M, Werner ER, Mayer B, et al. Characterization of the inducible nitric oxide synthase oxygenase domain identifies a 49 amino acid segment required for subunit dimerization and tetrahydrobiopterin interaction. Biochemistry 1997;36(35):10609-19.
35. Raman CSL, H. Martasek, P. Kral, V. Masters, B.S. Poulos, T.L. Crystal structure of constitutive endothelial nitric oxide synthase: a paradigm for pterin function involving a novel metal center. Cell 1998;95:939.
36. Perera I, Bayachou M. Manuscript in preparation.
37. Sauerbrey G. The use of quartz oscillators for weighing thin layers and for microweighing. Zeitschrift fuer Physik 1959;155:206-22.

38. Schnell ZBVL, A.M. Kranpitz, T.R. Amino Acid Screen, Blood. In: F.A.Davis, editor. Davis's comprehensive handbook of Laboratory and diagnostic tests with nursing implications; 2003.
39. Clague MJW, J.S. Marletta, M.A. Formation of N-cyanoornithine from N-hydroxy-L-arginine and hydrogen peroxide by neuronal nitric oxide synthase: implications for mechanism. Biochemistry 1997;36:14465-14473.
40. Stuehr DJK, N.S. Nathan, C.F. Griffith, O.W. N-hydroxy-L-arginine is an intermediate in the biosynthesis of nitric oxide from L-arginine. J Biol Chem 1991;266(10):6259-6263.
41. Lenormant H, Blout ER. Origin of the absorption band at 1,550 cm.-1 in proteins. Nature 1953;172(4382):770-1.
42. Crane BR, Arvai AS, Gachhui R, Wu C, Ghosh DK, Getzoff ED, et al. The structure of nitric oxide synthase oxygenase domain and inhibitor complexes. Science 1997;278(5337):425-31.
43. Jun H-W, Taite LJ, West JL. Nitric Oxide-Producing Polyurethanes. Biomacromolecules 2005;6(2):838-844.
44. Miller PE, Carlton D, Deierhoi MH, Redden DT, Allon M. Natural history of arteriovenous grafts in hemodialysis patients. Am J Kidney Dis 2000;36(1):68-74.

45. Tamada Y, Kulik EA, Ikada Y. Simple method for platelet counting. Biomaterials 1995;16(3):259-61.

46. Tsai WB, Grunkemeier JM, Horbett TA. Human plasma fibrinogen adsorption and platelet adhesion to polystyrene. J Biomed Mater Res 1999;44(2):130-9.

47. Suggs LJ, West JL, Mikos AG. Platelet adhesion on a bioresorbable poly(propylene fumarate-co-ethylene glycol) copolymer. Biomaterials 1999;20(7):683-90.

CHAPTER V

CONCLUSIONS AND FUTURE DIRECTIONS

5.1 CONCLUSIONS

During the past century, the use of implantable medical devices and other blood contacting biomedical devices have evolved from a mere dream to a widely adopted medical practice, including the use of stents, vascular grafts, sensors, pacemakers, heart valves, hemodialyzers, extracorporeal circuits, and membrane oxygenators [1, 2]. However, one of the major problems associated with these devices, is that the introduction of such devices leads to injury of the blood vessel walls. Clot formation or thrombosis also results at the injured site, causing stenosis or occlusion of the blood vessel. Moreover, if the medical device is left within the patient for an extended period of time, thrombus

ultimately forms on the device itself, again causing stenosis or occlusion. The driving force behind these issues is the lack of hemocompatibility of the polymeric materials used to prepare such devices. The biocompatibility of an implantable medical device is defined as the ability of the device to perform its intended function, with the desired incorporation within the host, without eliciting any undesirable local or systemic effects in that host [3]. There exists a need for modification of medical devices, with materials capable of enhancing the biocompatibility of these devices from the first instance of blood and tissue contact to days or weeks following its first use. The best-known example of a completely non-thrombogenic surface is the vascular endothelium that lines the inner walls of all blood vessels. The biological responses underlining the biocompatibility of this lining are mediated by a number of active molecules that are either expressed at the surface such as heparan sulfate, and thrombomodulin [4], or are continuously being secreted such as prostacyclin, plasminogen, antithrombin III and Nitric Oxide (NO) [5].

NO releasing bio-polymers are being sought as effective anti-thrombotic coatings in an attempt to enhance thromboresistivity of those devices. The approaches utilizing NO-donors incorporated into polymeric

matrices suffer from being a finite NO reservoir, and thus they are limited in their ability to sustain NO fluxes over a prolonged period of time. The alternative is then to explore approaches that would lead to materials with the ability to sustain NO generation for longer durations and at levels comparable to stimulated human endothelial cells (0.5 - $4x10^{-10}$ $molcm^{-2}min^{-1}$) [6]. NOS based polyethyleneimine coatings were successfully developed with the layer-by-layer methodology. NO was successfully generated from these coatings at levels comparable to stimulated human endothelial cells. NO release from these coatings successfully decreased platelet adhesion at the surface by 60%, which leads to improved thromboresistivity of implantable devices when coated with those materials.

5.2 FUTURE DIRECTIONS

Various efforts have been made to prepare more blood compatible surfaces that include NO-release (anti-platelet activity), heparin bound (anticoagulant activity) [7], or thrombomodulin-immobilized polymeric coatings [8]. The potency of such materials in preventing clot formation may be limited to the fact that these materials

partially address the thromboresistivity issues. These materials possess partial thromboreisistivity (either anti-platelet or anticoagulant activity). The alternative could be the development of surfaces that integrates both anti-platelet and anticoagulant agents that will act synergistically to achieve higher thromboresistivity levels. The integration of a combination of the agents that possess anti-platelet and anticoagulant activity into a polymeric matrix in such a manner that they are either released or are immobilized on the surface should result in a 'truly' biomimetic coating that closely resembles the endothelial cell lining of the inner blood vessel wall.

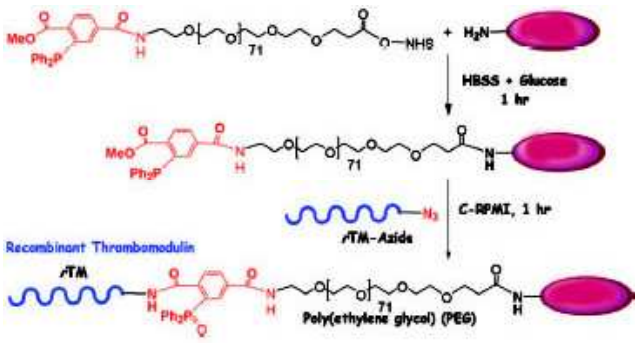

Figure 5.1: A schematic illustration of liposome surface glyco-functionalization through the Staudinger ligation. Adapted from [9]

Polymeric materials that combine NO release with surface-bound heparin have been developed in an initial effort to towards the fabrication of polymeric coating that truly mimic the endothelial cell functionality [10]. Thrombomodulin, a 74 kDa transmembrane protein acts as a modulator of thrombin activity *in vivo* [4]. Once thrombin binds to thrombomodulin on the endothelial cell surface, thrombin's fibrinogen cleaving activity is inhibited. In addition, the protein C anti-coagulation pathway is activated by this binding leading to the change of thrombin from a procoagulant state to an anti-coagulant state [11]. Multifunctional bilayer polymeric coatings have been recently described with both controlled NO release and surface bound active thrombomodulin or combined thrombomodulin and heparin that mimic the highly thromboresistant endothelium layers [12]. In addition, liposomes have been presented as candidates to prepare biomimetic coatings intended to enhance the biocompatibility of implantable medical devices [13]. Pancreatic Islets with recombinant azido-thrombomdulin were prepared by the chemoselective conjugation of an azido-functionalized thrombomodulin [14], to pancreatic islets by Staudinger ligation to a surface-bound bifunctional poly(ethylene glycol) linker (Figure 5.1). The presence of thrombomodulin on the surface was associated with a

significant increase in the production of activated protein C with a reduction in the islet-mediated thrombogenicity [9].

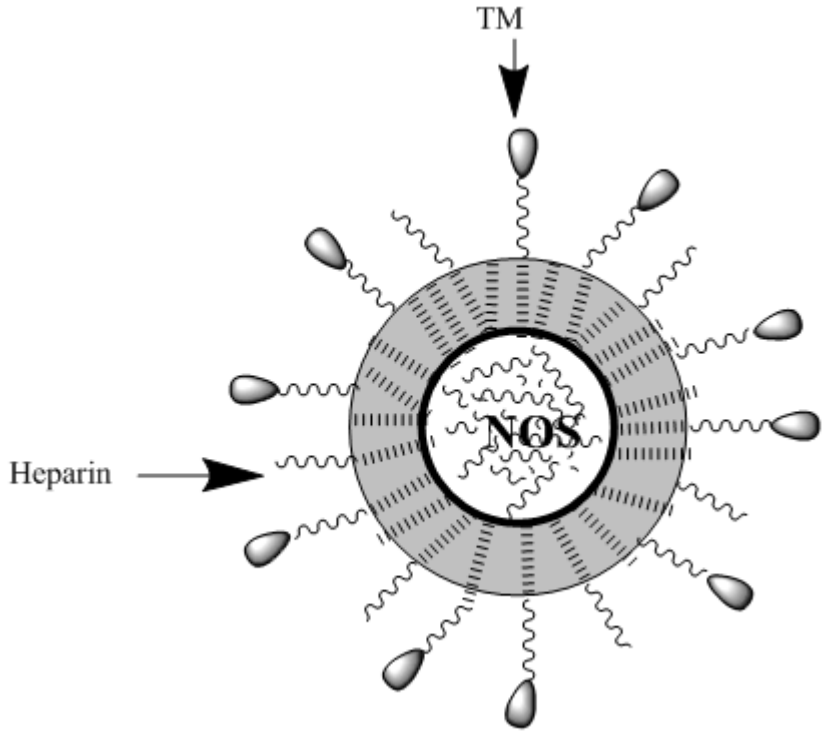

Figure 5.2: Schematic illustration of Liposomes that are capable of releasing Nitric Oxide with surface bound recombinant truncated thrombomodulin and heparin

Liposomes that are capable of releasing Nitric Oxide with surface bound thrombomodulin and heparin (Figure 5.2) appear to be a potential target to prepare biomimetic coatings that can be applied to surfaces of implantable medical devices to enhance their thromboresistivity and biocompatibility.

We demonstrate in this chapter the preliminary work involving the sub-cloning of a methionine-deficient thrombomodulin construct, followed by the subsequent expression and purification of the recombinant truncated thrombomodulin containing an azido-functionalized methionine analog as a C-terminal linker for site-specific functionalization using the Staudinger ligation [9].

5.2.1 Sub-cloning of Recombinant Truncated Thrombomodulin

A DNA fragment encoding for the truncated human thrombomodulin, containing N-terminal BAMHI restriction site and a C-terminal linker Gly Gly Met, was obtained by Polymerase Chain Reaction, by using the wild type thrombomodulin plasmid DNA as a template and primers Forward: 5'-GGATCCGTACCCTAACTACGACCTGGTG-3', and Reverse: 5'-

TTACATTCCACCTATGAGCAAGCCCGAATG-3'. The TOPO TA vector kit was used for the sub-cloning of the PCR products and the subsequent analysis of positive clones by restriction digestion using the BAMH I restriction enzyme. Site-directed mutagenesis was performed using primers Forward: 5'-CAGGTGCCAGCTGTTTTGCAACC-3' and Reverse: 5'-GGTTGCAAAACAGCTGGCACCTG-3' to generate a leucine (Leu) substitution for methionine-407 (M407L). The final construct (recombinant truncated thrombomodulin) was then inserted using the BAMHI site of the expression plasmid pET-39b(+) (Figure 5.3). The expression plasmid pET-39b(+) containing the recombinant thrombomodulin insert was sequence-verified and subsequently transformed into the E.coli methionine auxotroph B834(DE3).

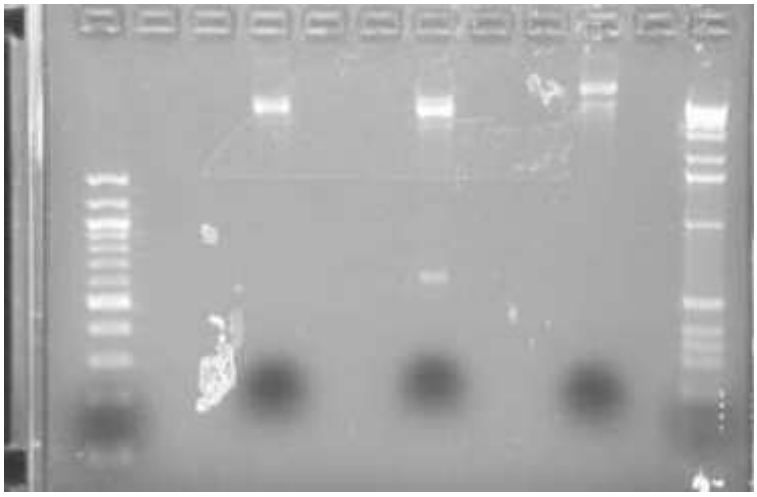

Figure 5.3: DNA gel electrophoresis depicting the size of the insert ligated with the pET-39b (+) plasmid.

5.2.2 Protein Expression and Purification

M9 minimal medium (500 mL), supplemented with 1 mM MgSO4, 0.4 wt % glucose, 1mg/L thiamine chloride, 0.1 mM $CaCl_2$, kanamycin (30mg/L), and all proteinogenic amino acids (40 mg/L), was inoculated with 20 mL of an overnight culture of the transformed cells. When the turbidity of the culture reached an OD600 of 0.8, protein expression was induced by addition of isopropyl-*â*-D-thiogalactopyranoside (IPTG) to a final concentration of 0.5 mM. After 5 min, the medium was exchanged to remove methionine, cells were sedimented (4000*g* for 20 min), and the cell pellet was washed twice with 200 mL of 1X M9 salts. Cells were resuspended in 500 mL of the M9 minimal medium described above, without methionine but supplemented with 100 mg/L of azido-functionalized methionine analogue. Cultures were grown for 4.5 h at 37 °C. The cells were first harvested by centrifugation at 4 °C at 10000*g* for 30 min and resuspended in 25mL of M9 buffer (1X M9 salts, 10% glycerol, 1 mg/mL lysozyme, and 10 μg/mL PMSF), and then the cells were lysed by sonication. The cell lysate was clarified by centrifugation at 10000*g* for 20 min. The supernatant was filtered through a 0.45μm syringe filters and then loaded onto a His-tag column. The presence of

thrombomodulin as an end product was confirmed using SDS-PAGE and quantified using S TAG rapid assay. Lane 5, features a band that corresponds to 36kDa in size confirming the presence of the truncated recombinant thrombomodulin. The average yield is 9.24mg of protein per liter of cell culture.

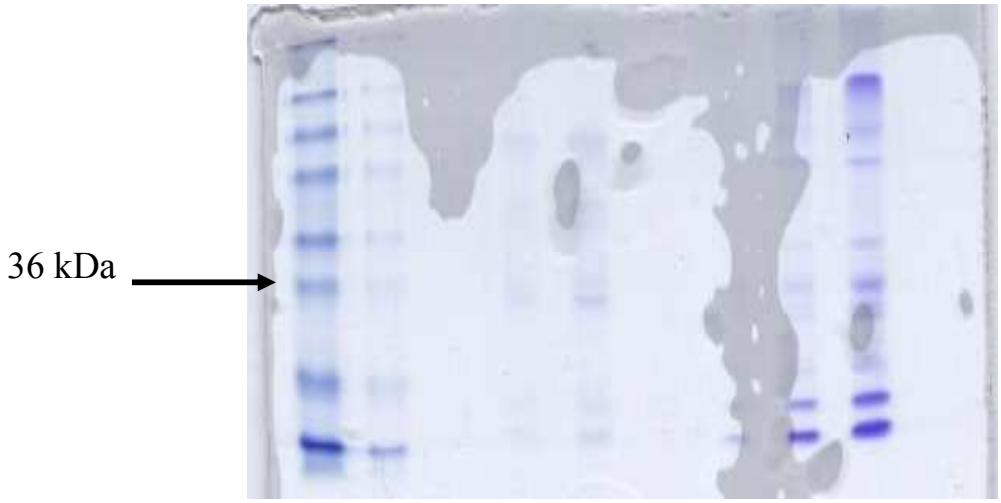

Figure 5.4: SDS PAGE of purified methionine deficient truncated recombinant thrombomodulin

5.3 REFERENCES

1. Peppas, N.A. and R. Langer, *New challenges in biomaterials.* Science, 1994. **263**(5154): p. 1715-20.
2. Ratner, B.D., *Blood compatibility--a perspective.* J Biomater Sci Polym Ed, 2000. **11**(11): p. 1107-19.
3. Williams, D., *Year-end perspectives: the introduction of new technologies.* Med Device Technol, 2003. **14**(10): p. 10-2.
4. Wen, D.Z., et al., *Human thrombomodulin: complete cDNA sequence and chromosome localization of the gene.* Biochemistry, 1987. **26**(14): p. 4350-7.
5. Coleman, R.W., *Mechanism of thrombus formation and dissolution.* Cardiovascular Pathology, 1993. **2**: p. 23S-31S.
6. Vaughn, M.W., L. Kuo, and J.C. Liao, *Estimation of nitric oxide production and reaction rates in tissue by use of a mathematical model.* Am J Physiol, 1998. **274**(6 Pt 2): p. H2163-76.
7. Wissink, M.J., et al., *Immobilization of heparin to EDC/NHS-crosslinked collagen. Characterization and in vitro evaluation.* Biomaterials, 2001. **22**(2): p. 151-63.

8. Sperling, C., et al., *Covalently immobilized thrombomodulin inhibits coagulation and complement activation of artificial surfaces in vitro.* Biomaterials, 2004. **25**(21): p. 5101-13.
9. Stabler, C.L., et al., *Surface re-engineering of pancreatic islets with recombinant azido-thrombomodulin.* Bioconjug Chem, 2007. **18**(6): p. 1713-5.
10. Zhou, Z. and M.E. Meyerhoff, *Preparation and characterization of polymeric coatings with combined nitric oxide release and immobilized active heparin.* Biomaterials, 2005. **26**: p. 6506-6517.
11. Sadler, J.E., *Thrombomodulin structure and function.* Thromb Haemost, 1997. **78**(1): p. 392-5.
12. Wu, B., et al., *Polymeric coatings that mimic the endothelium: combining nitric oxide release with surface-bound active thrombomodulin and heparin.* Biomaterials, 2007. **28**(28): p. 4047-55.
13. Valenzuela, S.M., *Liposome Techniques for Synthesis of Biomimetic Lipid Membranes*, in *Nanobiotechnology of Biomimetic Membranes*, D.K. Martin, Editor. 2007, Springer US. p. 75-87.
14. Cazalis, C.S., et al., *C-terminal site-specific PEGylation of a truncated thrombomodulin mutant with retention of full bioactivity.* Bioconjug Chem, 2004. **15**(5): p. 1005-9.